

75

AN ALKALIC CONTINENTAL VENT COMPLEX OF
THE DUBAWNT GROUP, N.W.T.

AN ALKALIC CONTINENTAL VENT COMPLEX OF
THE DUBAWNT GROUP, N.W.T.

by

KAREN JUDITH BAWDEN

Submitted to the Department of Geology
in Partial Fulfilment of the Requirements
for the Degree
Bachelor of Science

McMaster University
April, 1979

Bachelor of Science (1979)
(Geology)

McMaster University
Hamilton, Ontario

TITLE: An Alkalic Continental Vent Complex
 of the Dubawnt Group, N.W.T.

AUTHOR: Karen J. Bawden

SUPERVISOR: Dr. R. H. McNutt

NUMBER OF PAGES: vii; 69

SCOPE AND CONTENTS:

 An Alkalic suite of proterozoic volcanics and their associated sediments, situated within the Dubawnt Group of the Churchill Province, was mapped and studied. Petrography and geochemical analyses were performed on representative specimens. The extrusives and related dykes are thought to have been derived from the differentiation of a single parent magma, as evidenced by several geochemical trends. The units are as follows; intermediate to felsic trachytes and pyroclastics, typically phlogopite phyric and red alkali rhyolites; later volcanoclastic units. A significantly younger diabase dyke cuts these units, all of which overlie the '307' formation.

ACKNOWLEDGEMENTS

I wish to express my gratitude to the many people who assisted in the making of this thesis. I am particularly grateful for the assistance and encouragement provided by Dr. A. N. LeCheminant and Dr. M. B. Lambert of the G. S. C., initially during the summer field season, and later during the actual writing.

I would also like to thank my supervisor Dr. R. H. McNutt, for his guidance, his patience and his continued good humour.

Mr. Ota Mudroch performed the chemical analyses; Mr. Len Zwicker prepared the thin sections; Mr. Jack Whorwood provided assistance with the photography; and Mrs. Lynn Falkiner typed the manuscript. My thanks go to all of these people, and others at McMaster who provided help in many ways.

Last but not least, a short note of thanks goes to Lawrence, Randy and Ed who, surprisingly enough, provided stimulating and enlightening discussions throughout the year in room 308.

TABLE OF CONTENTS

	Page
CHAPTER ONE	
INTRODUCTION	1
Location and Accessibility	1
Previous Work	1
Field Work	2
General Geology	2
CHAPTER TWO	
FIELD RELATIONSHIPS	8
The Christopher Island Volcanics	9
CHAPTER THREE	
PETROGRAPHY	15
Syenites	16
Alkali Rhyolites	17
Phlogopite Trachytes	18
Pyroclastics	19
Volcaniclastics	20
CHAPTER FOUR	
CHEMICAL ANALYSES	29
CHAPTER FIVE	
Comparison with other Alkali Volcanics	41
CHAPTER SIX	
CONCLUSIONS	47
REFERENCES	51
APPENDIX	55

LIST OF FIGURES

Figure		Page
1	AFM Diagram	35
2	Selected Oxides vs. D.I.	36
3	Ab'-An-Or	37
4	Ol'-Ne'-Q' without 'LOI'	38
5	Ol'-Ne'-Q' with 'LOI'	39
6	$\text{Na}_2\text{O} + \text{K}_2\text{O}$ vs SiO_2	40
7	AFM Diagram comparing Nandewar Volcanics with Christopher Island Volcanics.	45
8	$\text{Na}_2\text{O} - \text{K}_2\text{O} - \text{CaO}$ Diagram	46

LIST OF PLATES

Plate		Page
1	Map of Dubawnt Group	6
2	Study Area with Sample Locations	7
3	Outcrop in Study Area	13
4	Agglomerate	13
5	Volcaniclastic	14
6	'307' Arkose	14
7	Syenite (t.s)	23
8	Phlogopite trachyte (t.s)	23
9	Glow banded alkali rhyolite (t.s.)	24
10	Flow banded alkali rhyolite (t.s.)	24
11	Bedded volcaniclastic (t.s.)	25
12	Volcaniclastic (t.s.)	25
13	Volcaniclastic (t.s.)	26
14	Volcaniclastic (t.s.)	26
15	Agglomerate (t.s.)	27
16	Volcaniclastic (t.s.)	27
17	Agglomerate (t.s.)	28
18	Agglomerate (t.s.)	28

CHAPTER ONE

INTRODUCTION

LOCATION AND ACCESSIBILITY

The study area lies to the west of Thirty Mile Lake on the Kazan River System, approximately 100 Km southwest of Baker Lake in the Northwest Territories.

Geographically, the area can be located on topographic map sheet "Thirty-Mile Lake" at longitude $97^{\circ}20'$ W and latitude $63^{\circ}35'$ N. The area mapped is roughly rectangular and covers approximately 60 Km^2 .

This somewhat remote area is accessible primarily by helicopter, and locally by boat along the Kazan River System. Access by fixed wing aircraft is limited to areas around the larger lakes, as the shallowness and swiftness of the Kazan River makes this approach somewhat hazardous.

PREVIOUS WORK

Work in the area in the past was limited to reconnaissance helicopter traverses during "Operation Baker" in 1955 and 1967, under G. M. Wright of the G.S.C. (Wright, 1955,1967).

In 1975, a more detailed mapping project was initiated by the G.S.C. under A. N. LeCheminant to map the west half of "MacQuoid Lake" map sheet and the east half of "Thirty-Mile Lake" map sheet. D. H. Blake has summarized much of this

work in "The Volcanic Rocks of the Dubawnt Group" (Blake, in press).

The mapping project was continued in 1978 with the mapping of part of the "Tebesjuak Lake" map sheet, and will be continued in 1979 with the mapping of an area to the east of Tulemalu Lake.

FIELD WORK

The field work, involving mapping and sampling was carried out during July of 1978. The initial traversing was accomplished during spotchecks of outcrops of the area. This was followed by a more detailed investigation of the Central region.

GENERAL GEOLOGY

The continental proterozoic deposits in the area to the southeast of Baker Lake constitute the Dubawnt Group of the Churchill Province. This group consists primarily of thick wedges of westerly dipping sedimentary and volcanic rocks, with the occasional high level intrusive body.

The Dubawnt Rocks rest conformably upon, or are in fault contact with, basement migmatitic granitoid gneisses, with thin interlayers of cataclastic leucocratic and mafic gneisses. Chlorite and epidote are generally common, both within veins and as an alteration product within the gneisses.

The overall trend of the foliation within this area is east to northeast, with younger diabase dykes trending parallel to subparallel to this foliation.

The as yet un-named basal sedimentary sequence has been correlated with the South Channel and Kazan formations, basal units to the northeast (Donaldson, 1965). For purposes of reference this formation will be referred to as the 307 formation.

The 307 formation consists of probable alluvial fan and fluvial deposits, with possible apparent thicknesses of 1500 m. This thickness is probably an over-estimate, as this formation is made up in part of overlapping clastic wedges. Although this unit varies locally, it is characteristically a massive to poorly bedded polymictic conglomerate with clasts of felsic gneiss and granodiorite up to 70 cm along their longest axes. The matrix is typically chloritic and maroon to light maroon in colour. The coarser base grades upward into a grey to light pink, medium grained arkose.

The 307 formation is overlain by alkalic lavas, pyroclastics and volcanoclastic sediments of the Christopher Island Formation. The suite of volcanics described in this thesis pertains to this formation. It is thought that the Christopher Island deposits were subaerial, with the occasional waterlaid pyroclastic and volcanoclastic, as evidenced by well developed bedding. Certain areas do show a wide variety of

well bedded volcanoclastic units that could indicate that some areas were locally low lying, if not subaqueous. Dessication cracks, lenses of conglomerate and volcanic slump deposits within some of the wacke units also suggest very shallow water. This will be discussed more fully in "Field Relationships".

Several different cycles of alkalic volcanic activity are thought to be represented by the Christopher Island Formation, each cycle being made up of mafic flows, felsic flows and pyroclastics. Representative units of such a cycle outcrop in the study area, though just how many cycles are present is not known. It is possible that the units represent one cycle, or possibly the end of one and the beginning of a second. This is deduced through comparison with several other cycles of volcanism as represented by units to the south west, and geological field relationships.

Dykes within the previously mentioned units include biotite lamprophyres and two types of syenite, one type showing a somewhat higher than normal uranium content. The syenite dykes appear to be contemporaneous with the felsic flows.

As shown in Plate 1 the Christopher Island Volcanics are overlain in several areas by minor deposits of volcanoclastic conglomerates, red sandstones and conglomerates.

They are poorly sorted, immature reddish grey deposits interpreted as wedges of alluvial fan sediments consisting of interbedded mudflow and stream channel deposits (LeCheminant, 1978).

The unconformably overlying Pitz formation consists of flow banded rhyolites, welded lithic crystal tuff and rhyolite-cobble conglomerates. Fluorite is a common accessory mineral within these rocks.

Overlying the Pitz calc-alkali volcanics are the sediments of the Thelon Formation, (LeCheminant, 1978) poorly bedded quartz-rich grit and conglomerate with a wide variety of clasts from the earlier formations.

All the preceding proterozoic rocks are intruded by leucocratic, red syenite stocks and miarolitic, fluorite bearing granite. These granites are thought to represent successive extrusive and high level intrusive events related to a single period of acid magmatism, with the Pitz volcanics. (LeCheminant, 1978).

PLATE 1: DUBAWNT GROUP, BAKER LAKE
DISTRICT OF KEEWATIN

Study Area

(after A. N. LeCheminant, 1978)

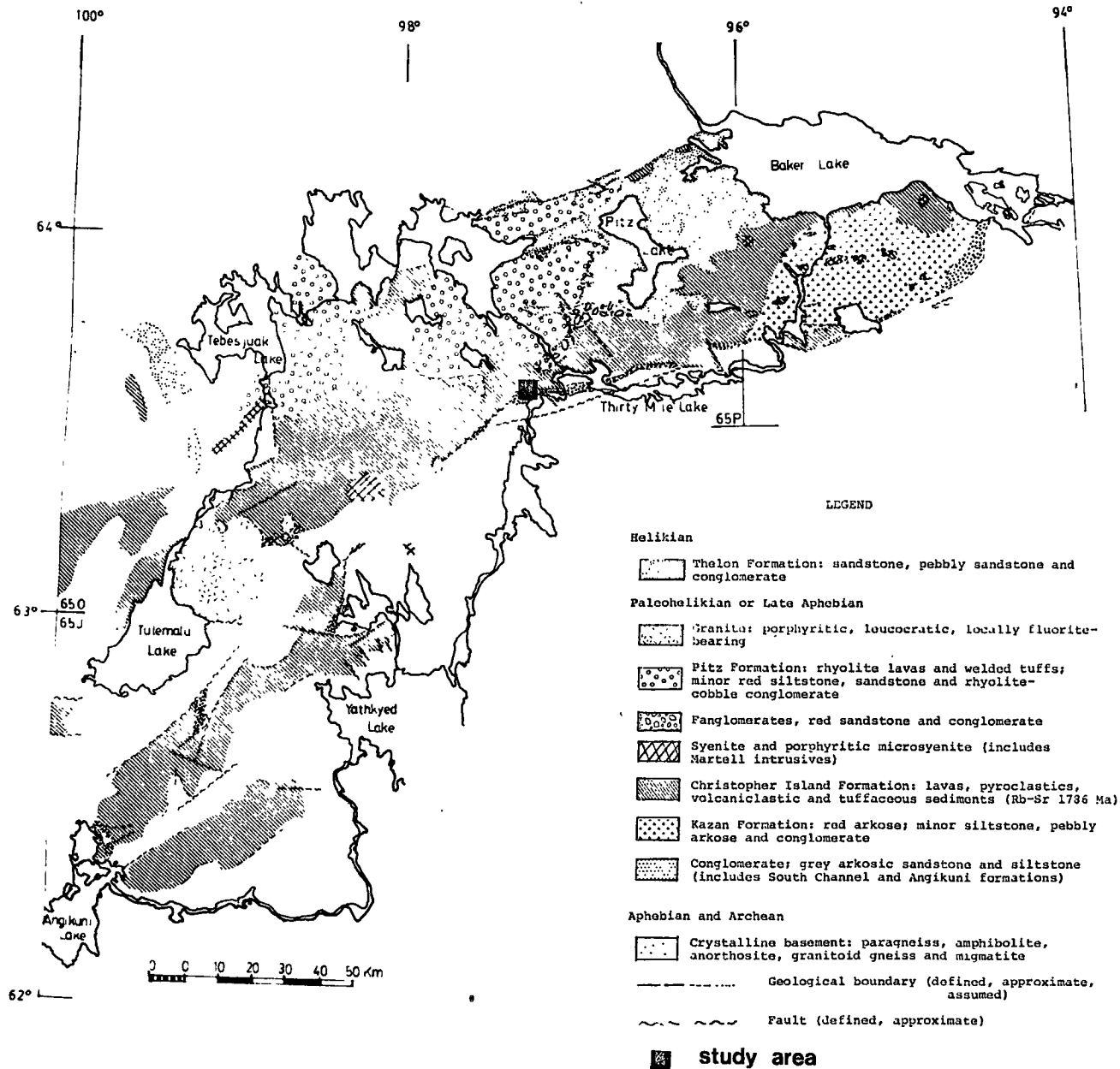


PLATE 2: STUDY AREA WITH SAMPLE LOCATIONS



CHAPTER TWO

FIELD RELATIONSHIPS

The arkose in the study area corresponds to the upper part of the 307 formation. The 307 formation, within the study area shows gentle folding in the south end of the study area, and is locally unconformable with the overlying Christopher Island Volcanics.

The arkose varies significantly in its appearance over relatively short distances, from typically pale grey to green, fine to medium grained deposits, to pale pink and white, medium to coarse grained deposits that are somewhat more silicified and sericitized.

The white coloured arkose appears to be somewhat more highly indurated giving the rock an atypical quartzite appearance in outcrop. In this location it corresponds to the upper 80-100 m of the formation and is thought to represent an alteration zone along an east-northeast fault which cross cuts the northern limits of the area mapped (Le Cheminant, 1978). A similar white arkose was formed to the southwest, also thought to correspond to an alteration zone along a major fault. The colour change appears to be gradational and pre-volcanic activity, associated with faulting and associated fluids. (personal communication, LeCheminant, 1978).

The author, however, suspects that due to the close

association of the altered zone with the agglomerate, which in turn is closely related to the immediate vent area, the alteration may be contemporaneous with volcanic activity and its associated hydrothermal fluids. Likewise the altered area mapped to the southwest could be the result of volcanogenic alteration, and possibly this zone also corresponds to a vent area. It is unlikely that the white arkose reflects a facies change as basement clasts found within the rock are also now bleached. (Plate 6).

Conglomeratic beds with rounded cobbles and gneissic basement pebbles occur within the arkose typically upon scour surfaces. Shale rip-ups were also observed locally, an indication of shallow water conditions. Bedding was rarely seen but this is likely due to the nature of the weathered surface, as several frost-heaved blocks show excellent laminar bedding along fresh fracture surfaces where lichen growth is minimal. The occasional tabular cross stratification was observed up to 25 cm in thickness.

THE CHRISTOPHER ISLAND VOLCANICS

Among the problems encountered during mapping was the apparent variety of rock types, and the complexity of their contacts. For this reason flow rocks and dyke rocks could not always be distinguished. The flow rocks and intrusives of the area were classified, in the field, on the basis of

phenocrysts and crystallinity of the groundmass. The predominant flows of the area are the distinctive red feldspar-phyric trachytes. Flow banding, flow-top breccias and chilled margins are evident in certain localities.

The more mafic flows are commonly dark grey green to maroon and contain a higher percentage of amphibole phenocrysts along with the white euhedral feldspars.

The feldspar-phyric syenites of the area are generally found as relatively large dykes cutting the earlier flows. They too are quite distinctive, as they contain dark grey zoned K-spar phenocrysts which are more resistant to weathering than the groundmass. These dykes also occur within the 307 formation, and are generally quite large, up to 3 m wide in these instances. The dykes are quite homogeneous throughout the area.

The overlying phlogopite-phyric trachytes are dark green in colour and are often difficult to distinguish from contemporaneous tuffs. Unlike the felsic flows and syenite dykes these rocks are extensively carbonatized, evidenced in outcrop by the presence of numerous tiny calcite filled 'tension gashes'. This carbonate could occur as the result of a volatile rich explosive eruption supplying the required CO_2 .

One of the most impressive rocks in outcrop is the agglomerate, in this usage referring solely to pyroclastic

rocks containing volcanic bombs. The tuffaceous matrix weathers more readily than the large trachytic bombs and accidentals giving the outcrop a knobby appearance. The bombs show a characteristic weathering pattern, with small scale fractures about their rims, generally perpendicular to their long axes. Even the smaller lapilli show a strong preferred orientation, to the extent that it has the appearance of being deformed, with a cleavage developed in the matrix. This is undoubtedly the result of welding as the rocks are otherwise distinctly unmetamorphosed.

Accidentals include porphyritic volcanics, gneissic clasts, numerous quartz cobbles, and arkose blocks, one in particular measuring one square metre. This is probably a block of underlying 307 arkose, displaced during the explosive expulsion of the agglomerate. The accidentals are predominantly well rounded, implying extensive prior reworking. The agglomerate grades laterally into tuffaceous bedded volcanoclastics with the occasional bomb. The agglomerate has a restricted occurrence, central to the vent. This proximity is assumed due to the large size of the bombs found within the agglomerate up to three metres in length by 25 cm wide. (Plate 4).

Lapilli tuffs and tuffs make up only a minor percentage of the pyroclastic deposits. In general the majority of the fine ash and lapilli are mixed with large amounts of epi-

clastic material, and hence have been classified as volcaniclastics.

The volcaniclastics are generally devoid of bedding, vary from fine to coarse grained, and are essentially arkosic. Very fine grained matrix supported purple volcaniclastic wackes occur in well bedded relatively thick sequences.

Bedding is laminar, and consistent over large areas. These purple wackes are probably fluvial, perhaps representing shallow basin or lake deposits. They outcrop occasionally in a narrow band parallel to the strike of the volcanics. However, the dip of the wacke is inconsistent with the other sediments and volcaniclastics in the area. Although the strike is often similar, the dip is generally to the south, rather than the north. This could reflect local topographical variations at the time of deposition, or significant age differences, with the wacke being considerably younger, deposited upon the somewhat eroded volcanic pile.

PLATE 3: Frosted heaved, lichen covered outcrop in the
study area.

PLATE 4: Agglomerate showing large bomb in foreground;
many smaller bombs in background.

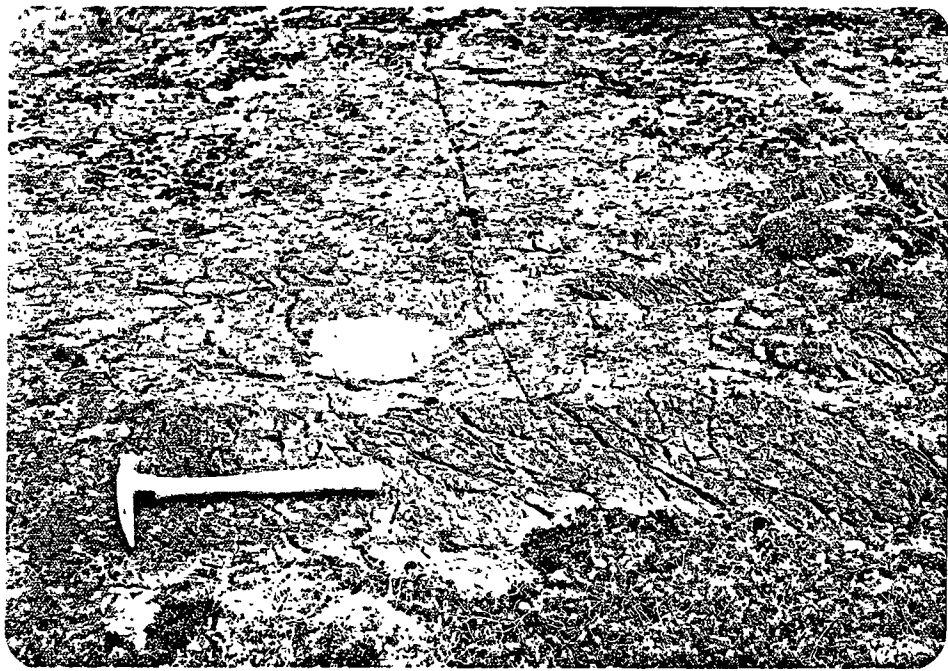


PLATE 5: Coarse scour deposits within a volcanoclastic
arkose, possible lahar type deposit.

PLATE 6: Bleached '307' arkose. Marking acts to designate
gneissic basement clasts.



CHAPTER THREE

PETROGRAPHY

Representative thin sections were obtained from each rock type observed in the field. In all 32 thin sections were examined, 21 from samples collected by the author and 11 from samples collected by A. N. LeCheminant.

The 307 formation, as mentioned in the field description can be further subdivided on the basis of alteration. Samples K17-1, K18-1, and T99-1 lie outside the altered zone, while K21-5, T120-2 and T103-1 are affected by alteration, being strongly carbonatized, sericitized and silicified.

The predominant grain size varies considerably from place to place, but degree of sorting and maturity appears to remain more or less consistent. The arkose is relatively immature and shows poor sorting with respect to grain size.

The clasts consist of quartz, plagioclase, perthite, microcline and other K-spars. There is a variety of polygonized quartzite grains from the archaean basement, some strained quartz grains and some composite lithic fragments. The grains range from subrounded to rounded along with some subangular grains. Depending upon stratigraphic location the arkose may be either matrix supported or clast supported. It should be noted that there are no volcanic

fragments visible in any of these samples, no phlogopite, nor brown microcline. These features are significant in determining the age relationships of the sediments with respect to the volcanic activity. Those deposited before the initiation of volcanism are devoid of phlogopite, brown microcline and volcanic fragments. Those deposited during and after volcanism contain varying proportions of these grains in direct relationship to the various stages of volcanic activity. The more extensive the alteration or reworking, then in all likelihood, the younger the unit in which they are found.

It is the matrix of the arkose which shows the carbonate alteration, particularly in the zones where the matrix is relatively more abundant along with substantial sericite in the matrix, there is also a small amount of pale green chlorite present, as stringers of fine grains between the clasts. Other minerals present in trace amounts are; epidote, as discrete grains within the fine grained matrix, opaques, biotite, subrounded zircons and apatite.

SYENITES

The syenites can be distinguished by their large euhedral to subhedral, zoned and commonly twinned K-spar laths. The pale brown K-spars are relatively fresh showing little sericitization. Both orthoclase and microcline are present,

with the rarer microcline displaying distinctive polysynthetic twinning.

The overall texture is hypidiomorphic granular with coarse interlocking feldspar laths, interstitial mafics and accessory minerals. The interstitial minerals include pale green slightly chloritized amphiboles, plagioclase showing albite twins, chlorite plates, slightly chloritized biotite plates, euhedral apatite, varying quantities of opaques with traces of epidote, carbonate and fluorite.

ALKALI RHYOLITES

The red alkali rhyolites and their slightly more mafic counterparts, the trachyandesites and trachybasalts are among the most common of the local rock types. The more felsic specimens sometimes show flow banding defined by aphanitic red layers with a finely crystalline mosaic of feldspar and quartz grains making up the majority of the groundmass. Large rounded slightly altered K-spar phenocrysts often display a glomeroporphyritic texture, shown to be distinct only by optical discontinuity under crossed nicols or sometimes irregular grain outlines (Plate 10). Most of these phenocrysts show remnants of Carlsbad twins, particularly the smaller phenocrysts. Smaller plagioclase phenocrysts are also present, showing vague albite twinning.

Varying amounts of opaques, chlorite and carbonate

occur in these rocks, amphiboles are notably absent in the alkali rhyolites.

PHLOGOPITE TRACHYTES

The phlogopite bearing trachytes differ mineralogically and texturally quite markedly from the previously described alkali rhyolites, trachytes and syenites. The predominant phenocryst is phlogopite, often with opaque reaction rims. As well, phlogopite constitutes a large proportion of the groundmass along with microcrystalline feldspar grains, giving it a pale yellowish brown tinge, distinctive of this rock type. This mineral is referred to as phlogopite after analysis by the G.S.C. of the same mineral in similar rocks of the region.

Large augite phenocrysts also occur in one of the sections, showing excellent twinning. Opaques are present in anomalously large amounts, in quantities found in no other rock type in the area. This rock type is the same as the volcanic bombs and lapilli found in the pyroclastics (Plate 8) implying contemporaneous effusion.

Carbonate alteration is ubiquitous and involves all mineral phases. Commonly large areas of the trachytic groundmass are obscured by irregular zones of coarse interlocking grains of calcite.

A flow orientation is relatively well defined by

subparallel alignment of phlogopite phenocrysts.

PYROCLASTICS

None of the pyroclastic sections studied are totally devoid of clastic material, rarely is there less than 10 % epiclastic content. The epiclastic material present is most commonly quartz showing undulose extinction. Composite grains are also present; also feldspar, often showing twinning, both microcline and albite.

The extent to which this material is epiclastic or pyroclastic is somewhat of a problem, it is apparent that even the cleanest pyroclastics have, to a certain extent, been subject to contamination from outside sources.

Of the crystals and fragments that are definitely volcanogenic are pale brown phlogopite plates, surprisingly fresh and unaltered, sometimes showing bending, particularly those plates perpendicular to the eutaxitic foliation, the result of compression during welding.

There are also some obvious fragments of larger zoned K-spar crystals, traces of which are a distinctive brown colour, a colour associated only with the volcanogenic K-spars.

Phlogopite trachyte fragments are common within the pyroclastics, varying widely in size and shape, they were apparently introduced in a semi-molten state. This is obvious in the case of the large fragments in outcrop which

have a characteristic bombshape. Smaller fragments, lapilli, show indistinct rounded edges in thin section (Plate 17).

One sample (T109-1) shows an additional type of lapilli fragment, an amphibole and phlogopite-phyric trachyte. The phlogopite is fine grained and relatively unaltered, the amphibole could be the soda-amphibole richterite, more extensive microprobe testing would be required for definite identification. The groundmass of the lapilli is composed of microcrystalline needles of colourless amphibole, K-spar and phlogopite. The colourless amphibole also occurs as part of the rock matrix as fine subhedral grains.

VOLCANICLASTICS

The volcaniclastics, in keeping with the other rock types also show considerable variation in grain size, sorting and clast to matrix ratio. Volcanic derived material includes phlogopite plate, lapilli of various types, including phlogopite trachyte fragments, devitrified shards, ash and the diagnostic brown K-spar fragments.

Volcanic material varies in the extent to which it has been reworked, from shards and fragments that were obviously molten upon deposition, due to their lensitic nature, to well rounded brown K-spar crystals.

Other than the volcanic material the clastic portion of the rock is not unlike that of the 307 formation in most cases, and probably reflects a continued supply from the

same source area.

Quartz, both strained and composite grains; feldspars, including twinned plagioclase, perthite and weakly sericitized K-spar grains are generally subrounded to rounded. In the cases where there is a high degree of angularity the source is probably volcanic.

Both clast supported and matrix supported samples were observed. In samples where ash makes up a part of the matrix, often as lenses, a eutaxitic foliation is apparent. Bedding is commonly evident on the microscopic scale, defined by small variations in grain size.

The matrix consists of silt-sized material with various concentrations of chlorite, epidote and carbonate, which is often extensive, particularly in those richest in volcanogenic material. Opaque content varies from traces to 10%, and appears to be related to the pyroclastic content.

The fine grained wackes are probably distal equivalents of the aforementioned volcanoclastics, as they too show rare volcanogenic material including the occasional phlogopite plate. They are extremely rich in fine grained opaques, indicating that although the environment was probably relatively calm, due to the laminar bedding, currents were sufficient to carry such heavy minerals, perhaps indicating turbidite type deposits or a nearby fluvial source, entering into a large basin.

Due to the proximity of other vent areas, one in particular to the east of the study area, intermixing of clastic material, was probably extensive. Therefore volcanoclastic material in the study area may not necessarily have originated from the local vent, and in all probability could cause the appearance of shards and other pyroclastic material in the study area, while that vent was actually quiescent.

PLATE 7: Syenite; large pale brown zoned k-spar lath in
centre with smaller laths to upper left and
interstitial epidote, chlorite and carbonate
(crossed nicols - 25x)

PLATE 8: Typical phlogopite trachyte; shows large opaque
rimmed phlogopite with high percentage of
disseminated opaques in groundmass.
(uncrossed nicols - 63x)

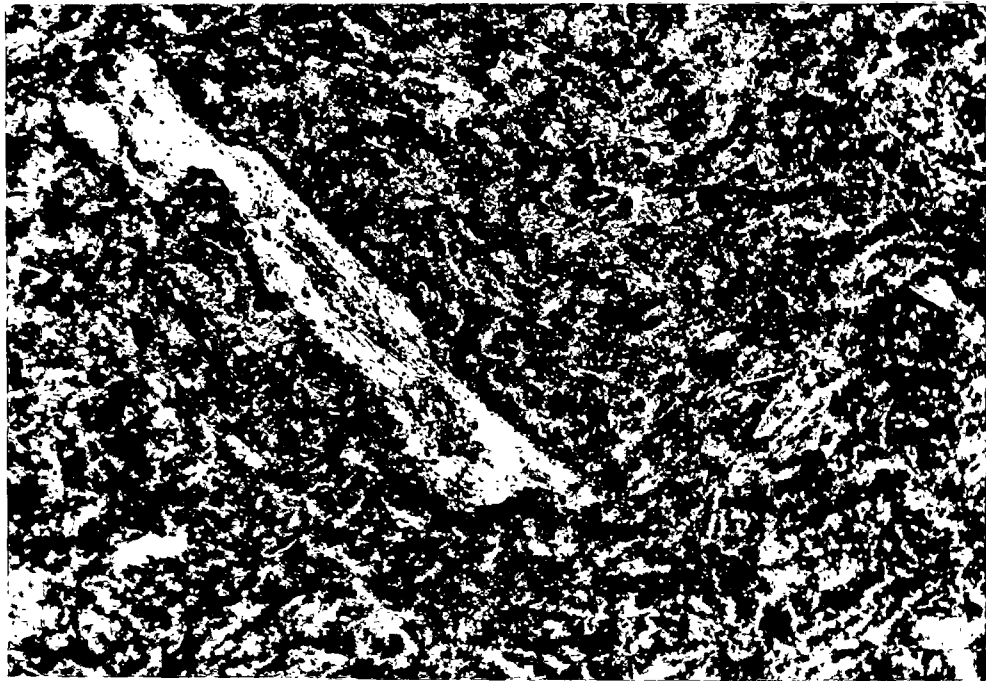


PLATE 9: Flow banded alkali rhyolite showing glomerophyric
texture. (Aphanitic bands are deep red)
(uncrossed nicols - 25x)

PLATE 10: Same flow banded alkali rhyolite as above, note
rounded clusters of zoned k-spar crystals to left.
(uncrossed nicols - 63x)

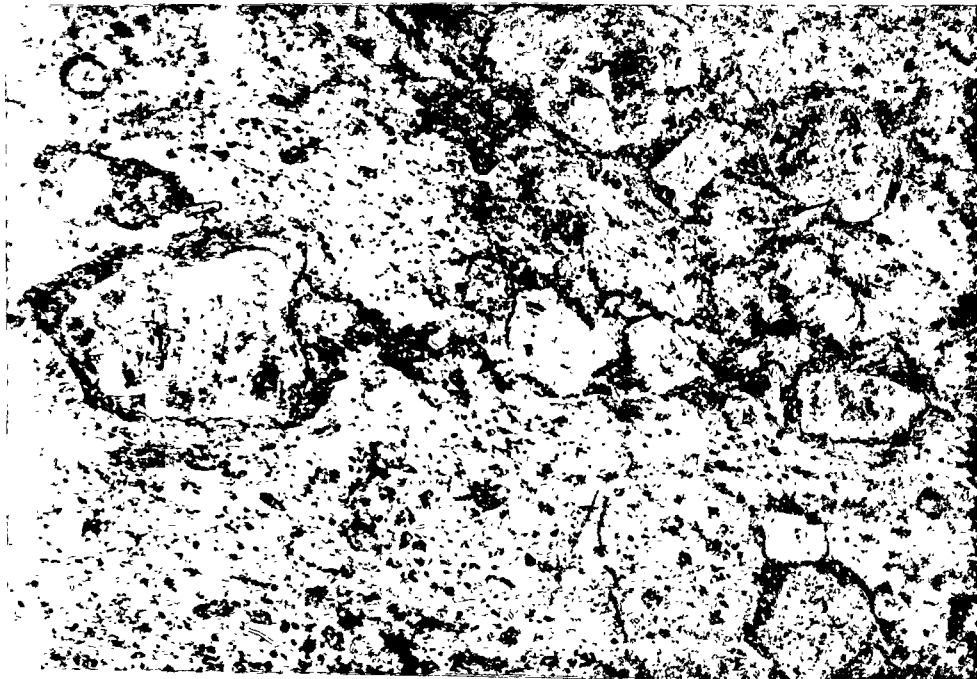
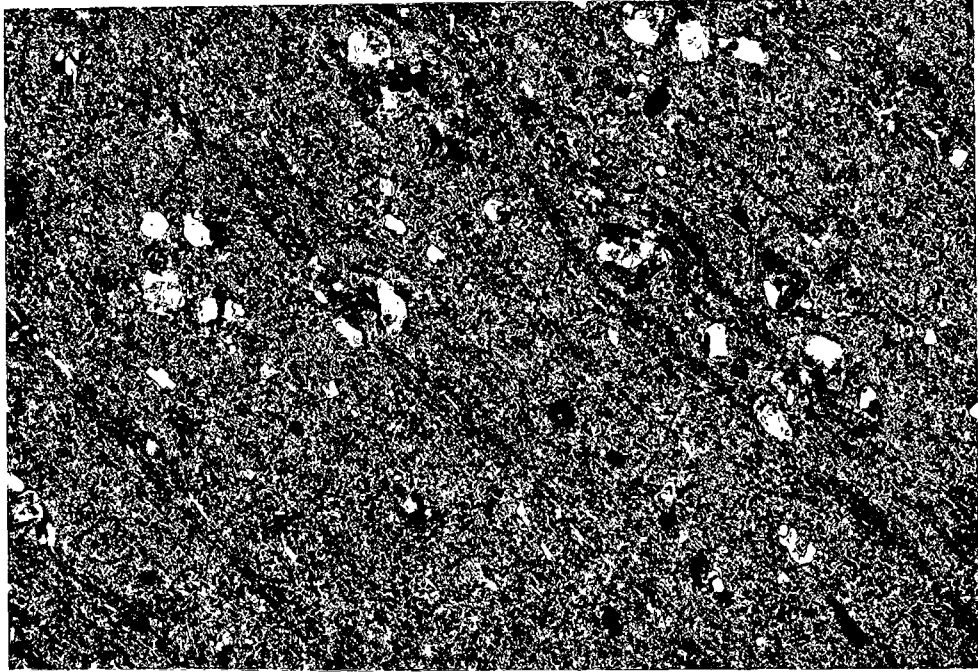


PLATE 11: Bedded volcanoclastic arkose; exceptionally high percentage of subrounded brown k-spar grains. Also, layer to top of photo contains a high percentage of aphanitic greenish ash.

(uncrossed nicols - 25x)

PLATE 12: Volcanoclastic; showing flattened pumice fragments moulded around epiclastic material. Also note the high percentage of ash in matrix.

(uncrossed nicols 63x)

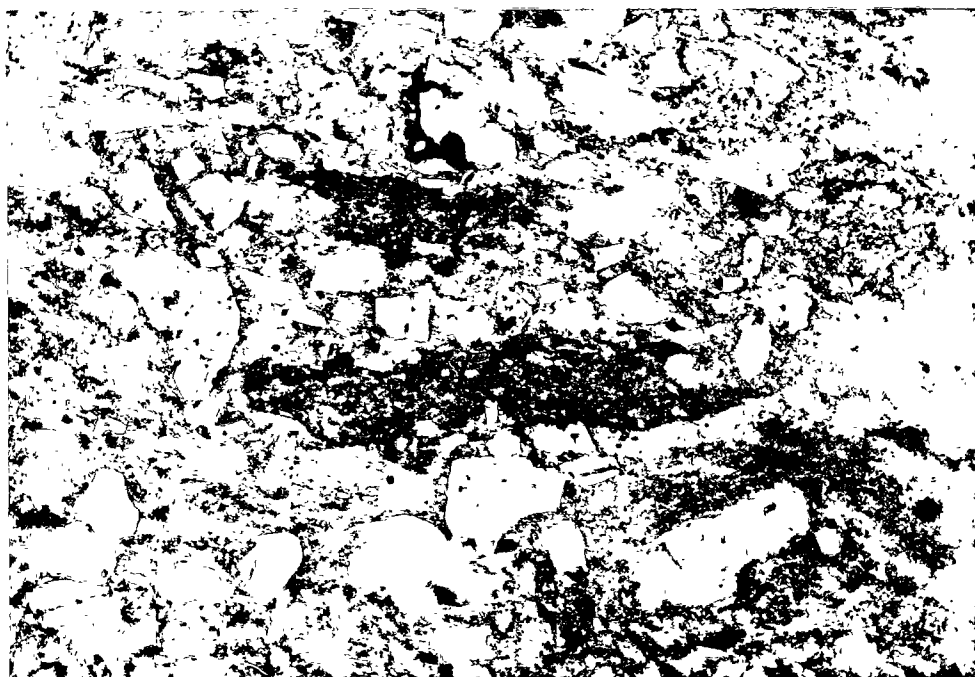
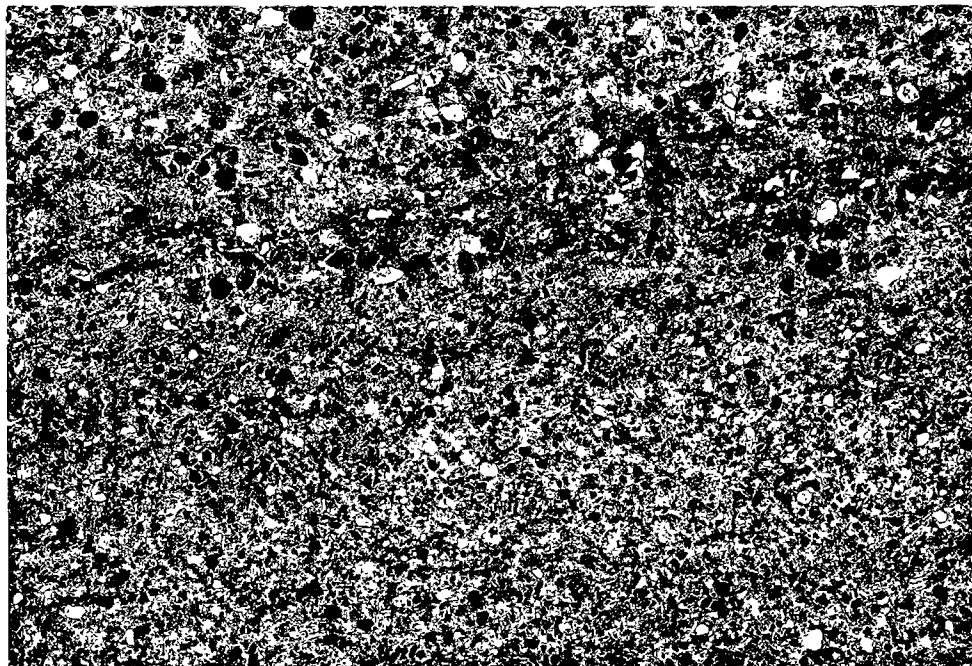


PLATE 13: Volcaniclastic; composed primarily of sub-
rounded phlogopite trachyte fragments showing
opaque reaction rims, siliceous matrix, no ash.
(uncrossed nicols - 25x)

PLATE 14: Volcaniclastic, two large phlogopite trachyte
clasts and numerous small well rounded clasts,
cut by quartz filled vein.
(crossed nicols - 25x)

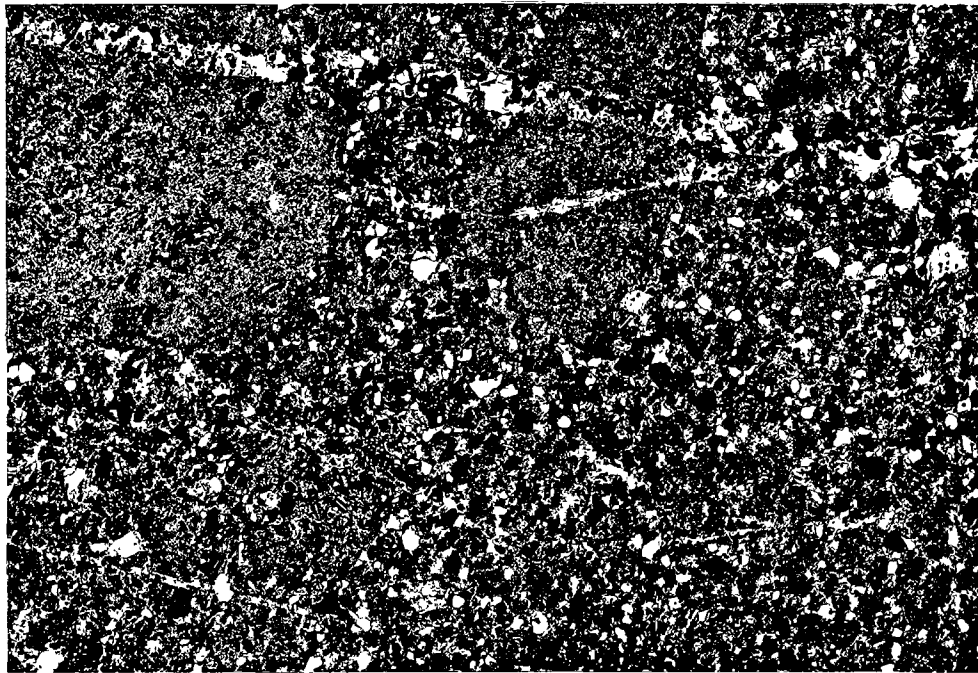
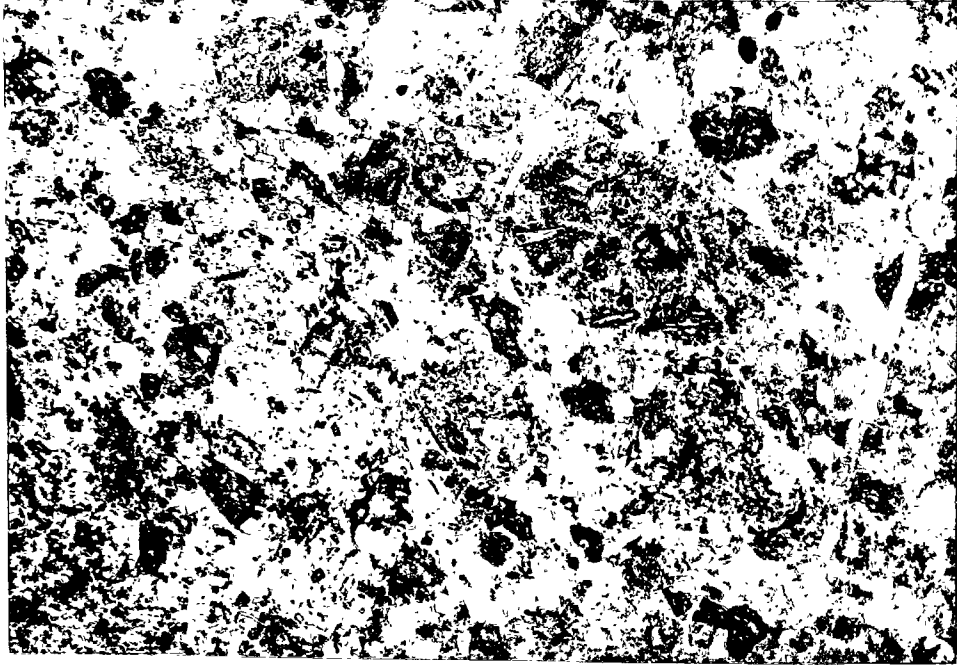


PLATE 15: Agglomerate; lower right portion of large
trachyte bomb and smaller lapilli, epiclasts
in ash matrix.

(crossed nicols - 25x)

PLATE 16: Ash-rich volcanoclastic; note large quartzite
grain to right of plate and lenses of ash
within matrix.

(crossed nicols - 25x)

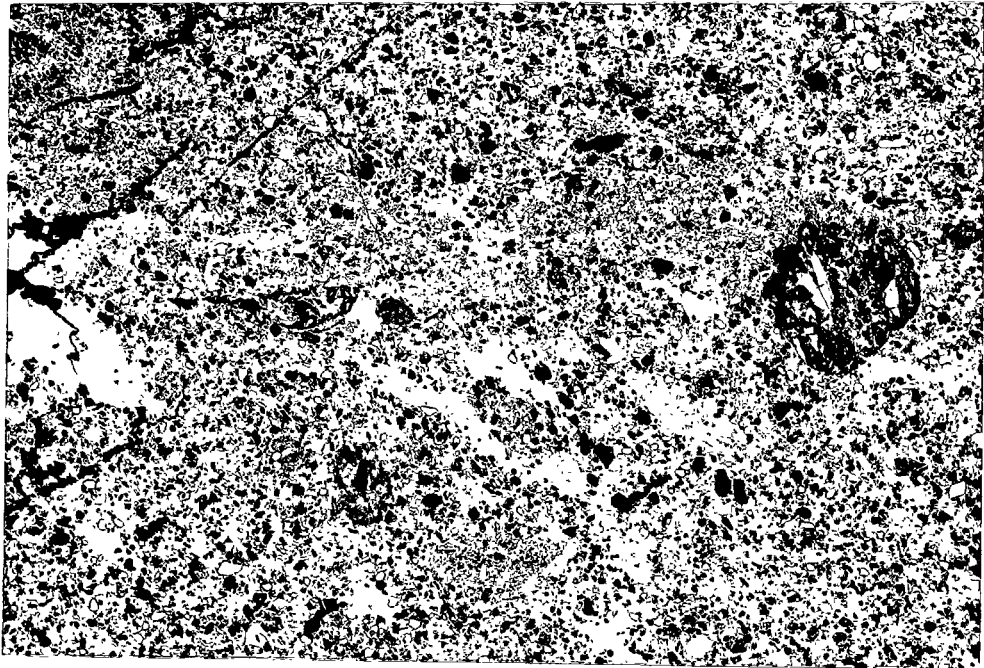
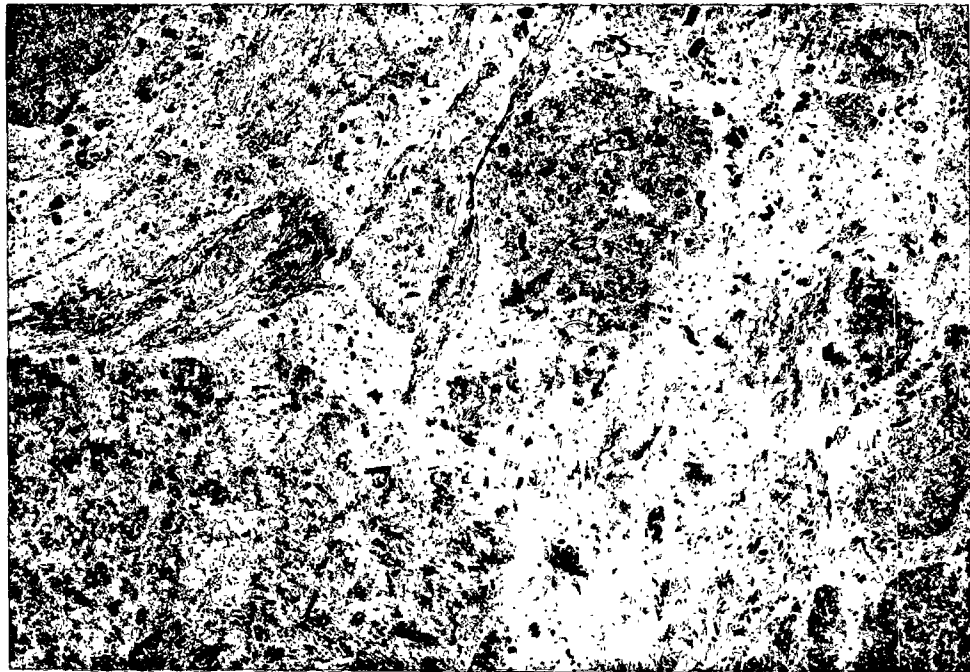
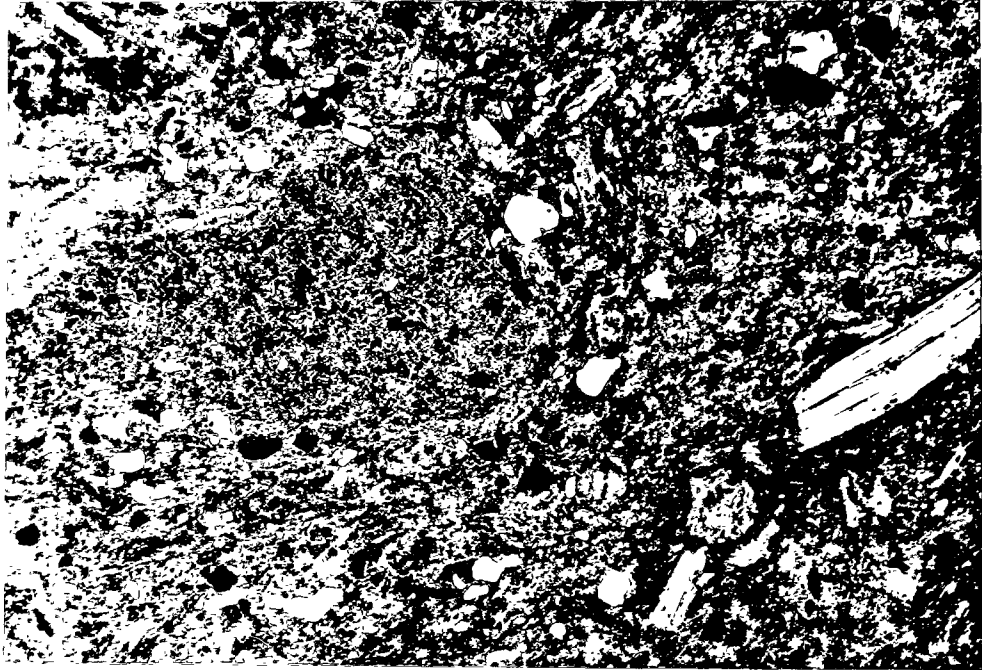


PLATE 17: Fragments within the Agglomerate; note phlogopite plate to right, volcanic fragment to left. Small white/grey grains are quartz and feldspar.
(crossed nicols - 63x)

PLATE 18: Phlogopite trachyte fragments in agglomerate with phlogopite plates showing opaque reaction rims, within aphanitic yellow-green ash matrix.
(crossed nicols-25x)



CHAPTER FOUR
CHEMICAL ANALYSES

The analysis of several representative samples of the igneous units was undertaken with some reservation, principally due to the nature of the alteration found in the area. The phlogopite bearing trachytes and pyroclastics are known, from thin section work, to contain significant amounts of carbonate. Also, many of the Christopher Island samples show traces of epidote, chlorite and sericite mineralization. Analysis of the pyroclastics other than the tuffs was ruled out due to obvious inhomogeneity of the samples. It should also be realized that the tuffs do not necessarily reflect the composition of the magmas from which they originated.

Whole rock, major and trace element analyses were done on the departmental XRF unit, a model 1450 AHP Philips machine. The trace elements analyzed were; Ba, Rb, Sr, Y, Zr and Nb.

To account for the carbonate content and H₂O, a loss on ignition (LOI) analysis was done. The powdered samples were heated to 900°C for 20 minutes in a muffle furnace, to drive off the volatiles.

The values obtained in this manner were then calculated with major and minor elements as CO₂ in one set of computer analyses. This is merely an approximation, as it also takes into account other volatiles present.

In what follows in the interpretations of the major and minor element data, both sets of results were applied, first for the C.I. P. W. norms and subsequently to the Irvine and Baragar program.

It should be noted that, due to the nature of the field relationships and the chemistry of the diabase sample, it will be considered separately.

The AFM plot (Fig. 1) shows a trend towards a relatively more significantly decreased iron and magnesium content in the more felsic flows. The plot is typical of an alkaline suite, (Irvine and Baragar, 1971).

The nature of the chemical trends with respect to the major elements is best visualized on a plot of weight percent oxide versus the Differentiation Index, (Fig. 2). This shows distinct relationships between the Differentiation Index (D.I.) and the weight percentages, particularly in the oxides of silica, magnesium and calcium, all of which plot as straight lines. Silica increases steadily with an increase in D.I., while both MgO and CaO steadily decrease with increasing D. I.

In the case of K_2O further data would be required to determine the exact trend. The six data points presently available are insufficient to positively determine whether K_2O is tending to increase or decrease. It appears to be decreasing slightly, especially within the range of D.I. equal to 80 - 100.

Sodium content increases with D. I., but not at a constant rate. Such trends are consistent with the hypothesis that the Christopher Island rocks of the study area are part of a single crystallization differentiation of a parent magma, ie. are related. Further samples of intermediate composition to the trachytes and alkali rhyolites might further substantiate this hypothesis.

The apparent gap in the trends between D. I. equal to 60 - 80 is most likely due only to restricted sampling. This gap is evident in most of the plots.

A plot of $Na_2O - K_2O - CaO$ (Fig. 8) supports a trend toward a relative decrease in CaO content along with a slight decrease in K_2O and slight increases in Na_2O contents, which is to be expected as this plot is merely a rearrangement of the previously plotted data.

The $Ab' - An - Or$ plot shows a compositional trend from orthoclase rich potassic trachytes to more sodic alkali-rich rhyolites, (Fig. 3). The diagram supports the potassic

nature of the samples, (Irvine and Baragar, 1971).

A further diagram, also applying the cation norm data is the OL' - NE' - Q' plot. This plot shows two distinct clusters of points, neither plotting significantly toward the alkaline area of the diagrams. The OL' - NE' - Q' plots are exceptional in that the data including 'LOI' results does not correlate with the data without 'LOI' included. The diagrams with 'LOI' plot well into the subalkaline area of the diagram, while without it, the rhyolites plot within the alkaline area. This results from significant changes which occur as a result of adding CO₂ to the norm analysis, which acts to change the distribution of elements between the various minerals. In effect, adding CO₂ significantly increases the quartz content, while all but eradicating the clinopyroxene, both of which figure significantly in this plot. Adding CO₂ also decreases AN, as the program with LOI calculates significant amounts of calcite.

The variation introduced by this factor results in a degree of uncertainty, this is considered in the final interpretation.

However, it is notable that the alkali rhyolites, regardless of the data used, plot from, at best borderline alkalic, implying differentiation toward a sub-alkaline composition.

A plot of $\text{Na}_2\text{O} + \text{K}_2\text{O}$ versus SiO_2 supports the $\text{Ol}' - \text{NE}' - \text{Q}'$ plot with the alkali rhyolites plotting close to the dividing line, on the subalkaline side, (Fig. 6). This diagram is not particularly useful in classifying the local samples.

It is also worthwhile to note that the data points for the pyroclastic sample do not vary significantly from those for the phlogopite trachyte, making adjustments for the epiclastic material results in an even closer correlation between the two, suggesting a similar source for both. The trace element data shows exceptionally high values of Si, Zr and Ba. This is typical of an alkaline magma. There is a significant enrichment of Ba in the tuff and the phlogopite trachyte as compared to the alkali rhyolites. This corresponds to a similar enrichment in orthoclase within the tuff and trachyte. It is probable that both Ba and Sr are substituting into the K-spar lattice.

The diabase dyke shows a comparable chemistry to that of the diabase dykes occurring as swarms in the Canadian Shield, as described by Fahrig and Wanless (1963). Fahrig and Wanless concluded that the diabase dyke swarms have intruded the shield frequently throughout the span of Pre-cambrian time, and that they were part of a much larger, volumetrically, event than is presently accounted for, as a consequence of erosion.

Not only does the chemistry of the diabase compare to that of the dyke swarms' but field evidence, specifically the strike of the dyke, correlates with that of other diabase dykes of the area.

Figure 1: AFM Diagram from Cation Norm Data

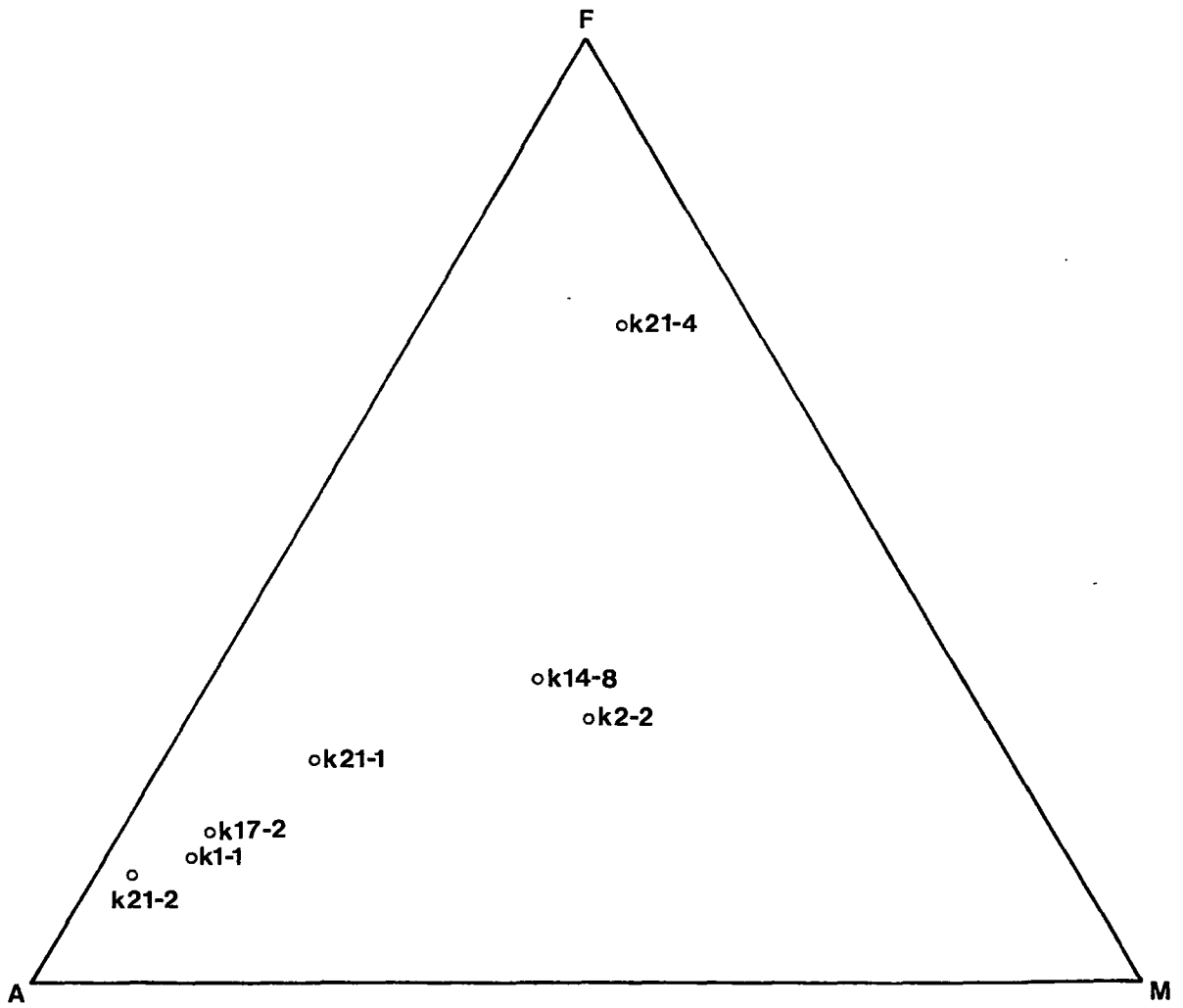


Figure 2: Selected Oxides Plotted Against Differentiation Index

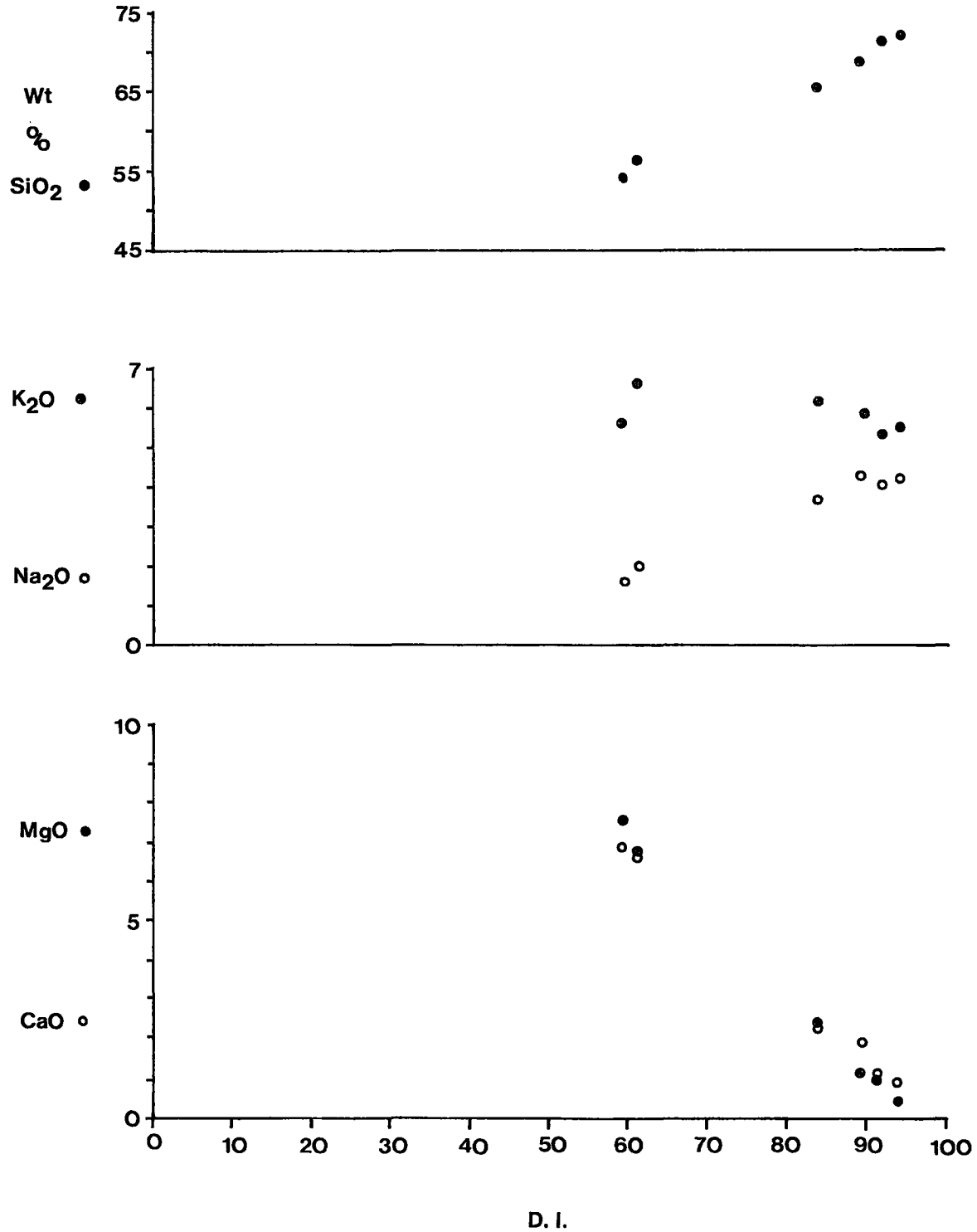


Figure 3: Ab'-An-Or Diagram from C.I.P.W. Norm Data

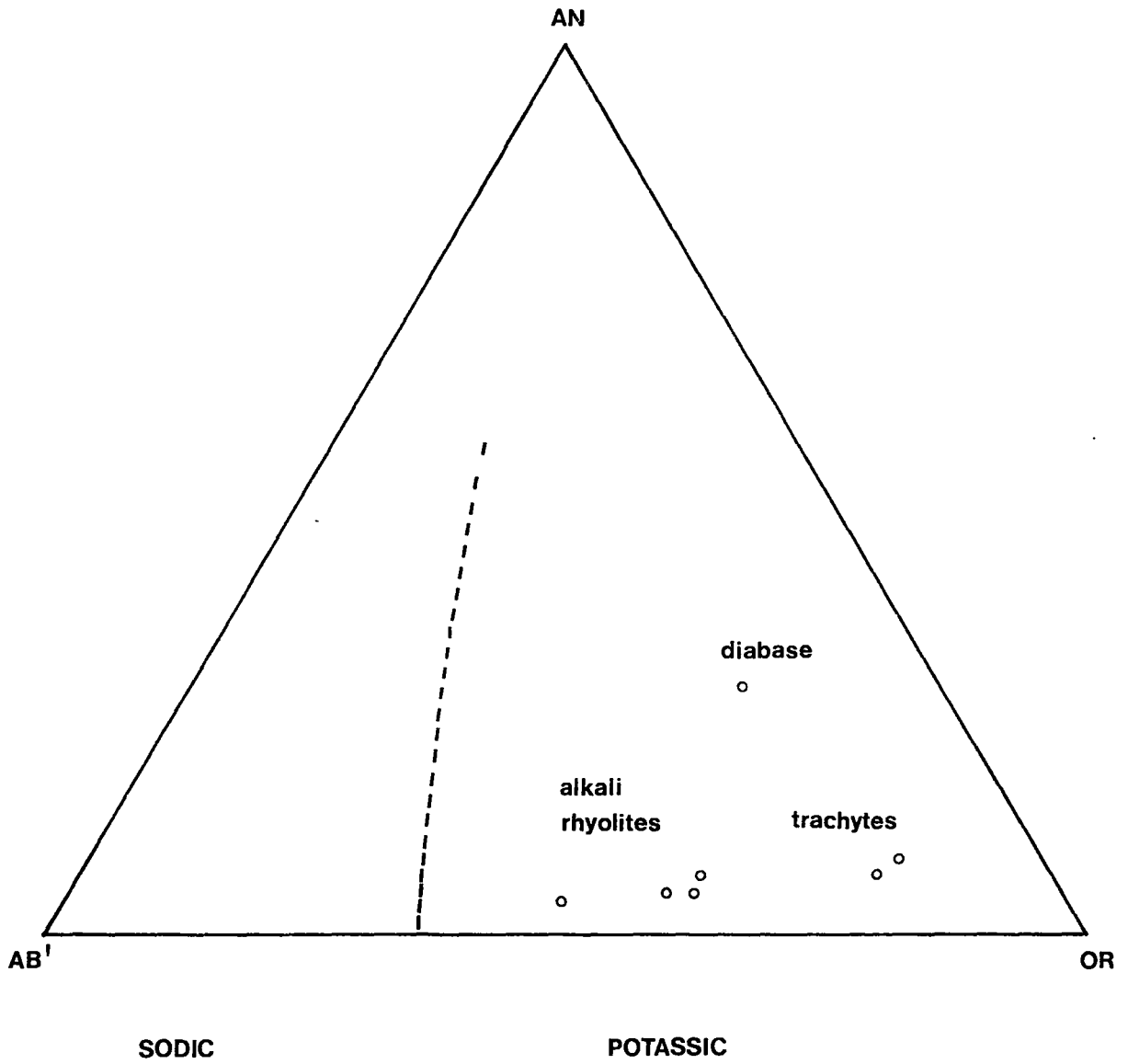


Figure 4: OL' - NE' - Q' without LOI

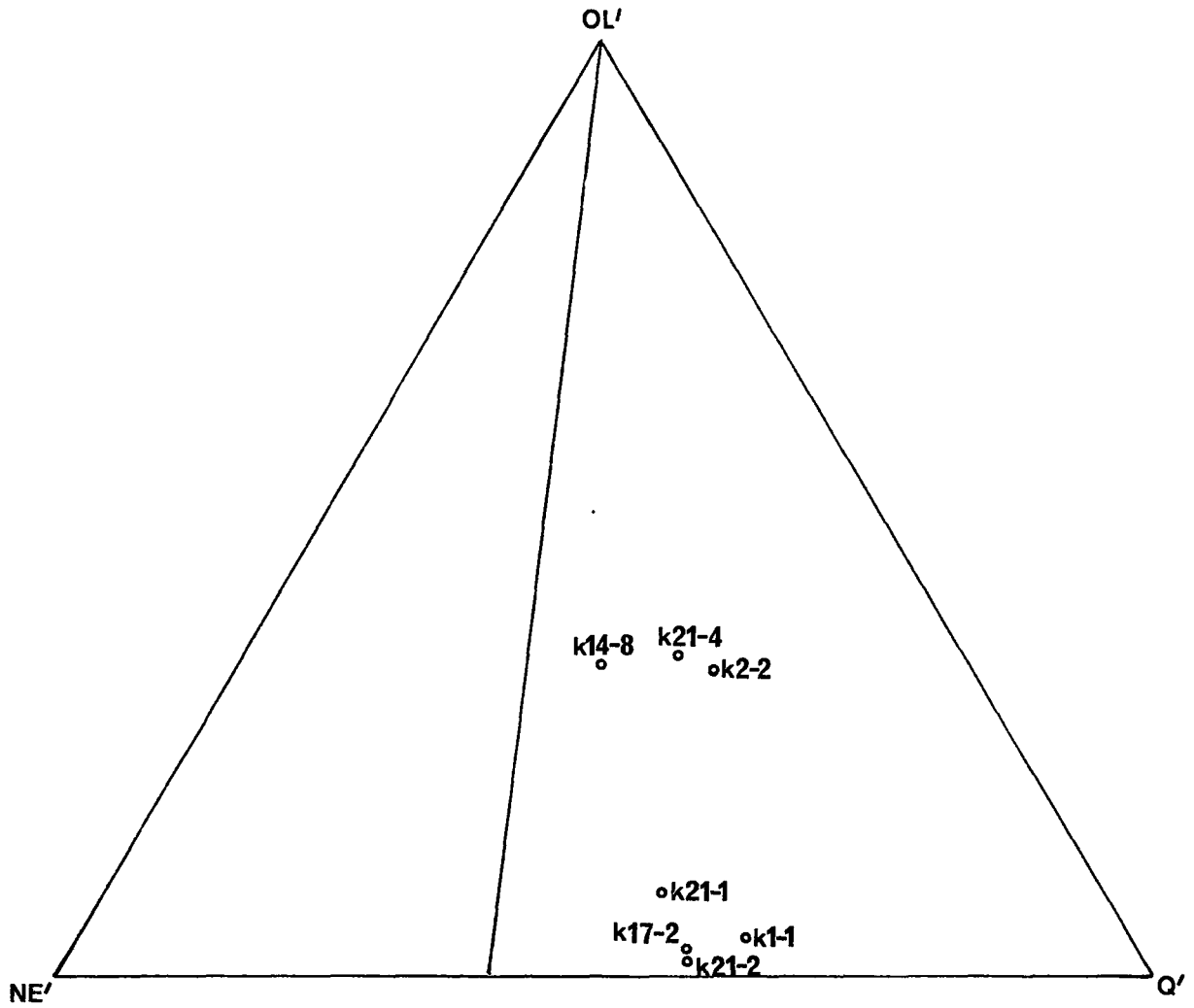


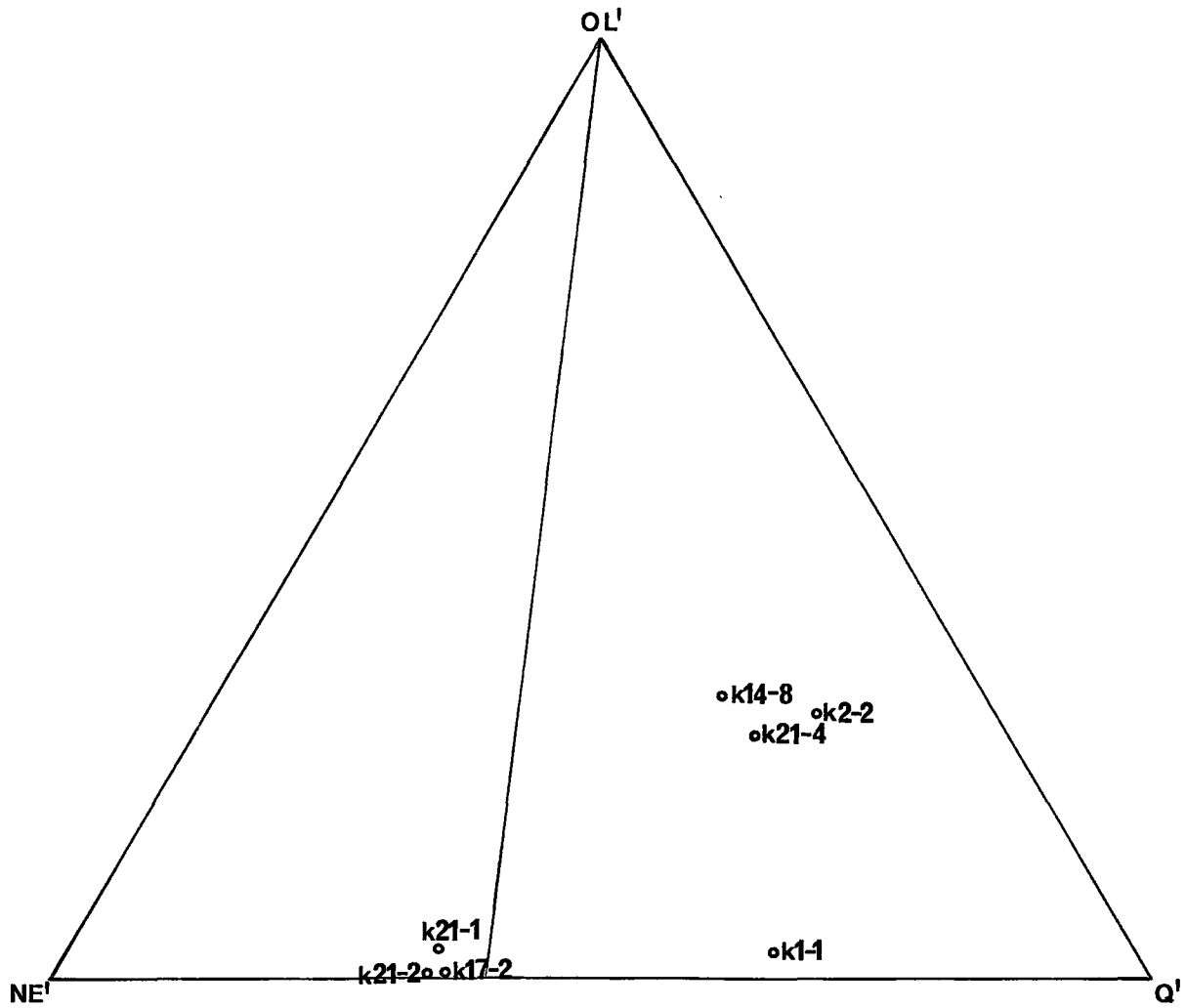
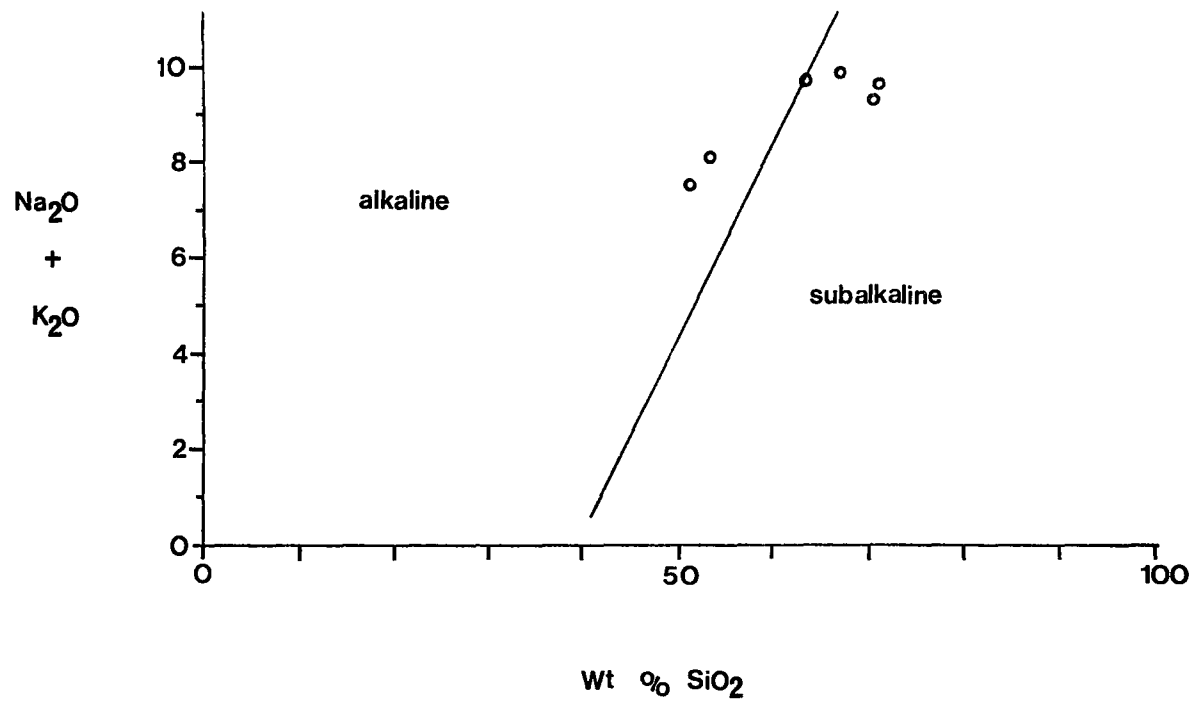
Figure 5: $OL' - NE' - Q'$ with LOI

Figure 6: $\text{Na}_2\text{O} + \text{K}_2\text{O}$ vs SiO_2



CHAPTER FIVE

COMPARISON WITH OTHER ALKALI VOLCANICS

Comparison of the geochemical data with that of other alkalic suites revealed very few other centres with similar chemistry at both the major and minor elements level. It became apparent, with the initial comparisons that, due to the wide variations in chemistry within the local samples, the samples could not be compared as a continuous suite, but instead as two discrete groups.

The two groups could not be matched simultaneously to any of the volcanic suites studied in the literature. When the rhyolites were comparable at a certain locality, there was not a comparable trachyte at the same location and vice versa. A division was made between the felsic alkali rhyolites and the significantly more mafic trachytes. This division was based primarily upon the clustering of points as shown on the various ternary diagrams that were plotted, as previously described in Chapter 4.

The calc-alkaline nature of the diabase and also the nature of field relationships implies a totally unrelated genetic origin, and hence it is excluded from this comparison.

Knowing that the Dubawnt Group had previously been

determined to consist, at least in part, of a series of continental sedimentary and volcanic units, (Wright, 1967) the samples were primarily compared with other alkalic suites currently classified as continental.

This comparison revealed that most of the suites are significantly more aluminum rich, on the average showing 4% more Al_2O_3 (King, 1960, 1970; Wilcockson, 1964). This is the case for volcanics in Tahiti; in the East African Rift System, those of Eastern Uganda, Burringa, Toro Ankole and Kivu; and also for those previously described in Canada, (Currie, 1976). Discrepancies in carbonate content were also noted in many cases.

However, in the final analysis carbonate content was deemed an unreliable constituent to be used in comparison, due to the strong possibility that much of the carbonate was secondary.

A suite of volcanic rocks from the Nandewar Volcano, New South Wales, Australia was found to compare closely with samples from the study area, in particular the alkali rhyolites.

The Nandewar Volcano was first described by Jensen (1907) and has since been thoroughly documented by Abbott (1969). The volcano is miocene in age, and its products range from olivine basalts to comendites and alkali rhyolites. They show extreme fractionation of a relatively

differentiated alkali olivine basalt magma, saturated with silica, to yield extremely oversaturated peralkaline comendites and peraluminous alkali rhyolites. A comparison of CaO-Na₂O-K₂O, AFM diagrams and a plot of selected oxides against the Differentiation Index of the study area and the Nandewar Volcanics showed similar trends (Figs. 8,7). The only discrepancies are the somewhat higher K₂O values of the Christopher Island rocks, and the slightly higher Al₂O₃ and total iron values of the earlier more mafic Nandewar Volcanics, as compared to mafic rocks of the study area.

Both the alkali rhyolites of Nandewar and the study area are low in Al₂O₃. It is more difficult to compare the mafic volcanics, as only two mafic samples from the study area were chemically analyzed. Further sampling of this area would be required before further analogies could be made.

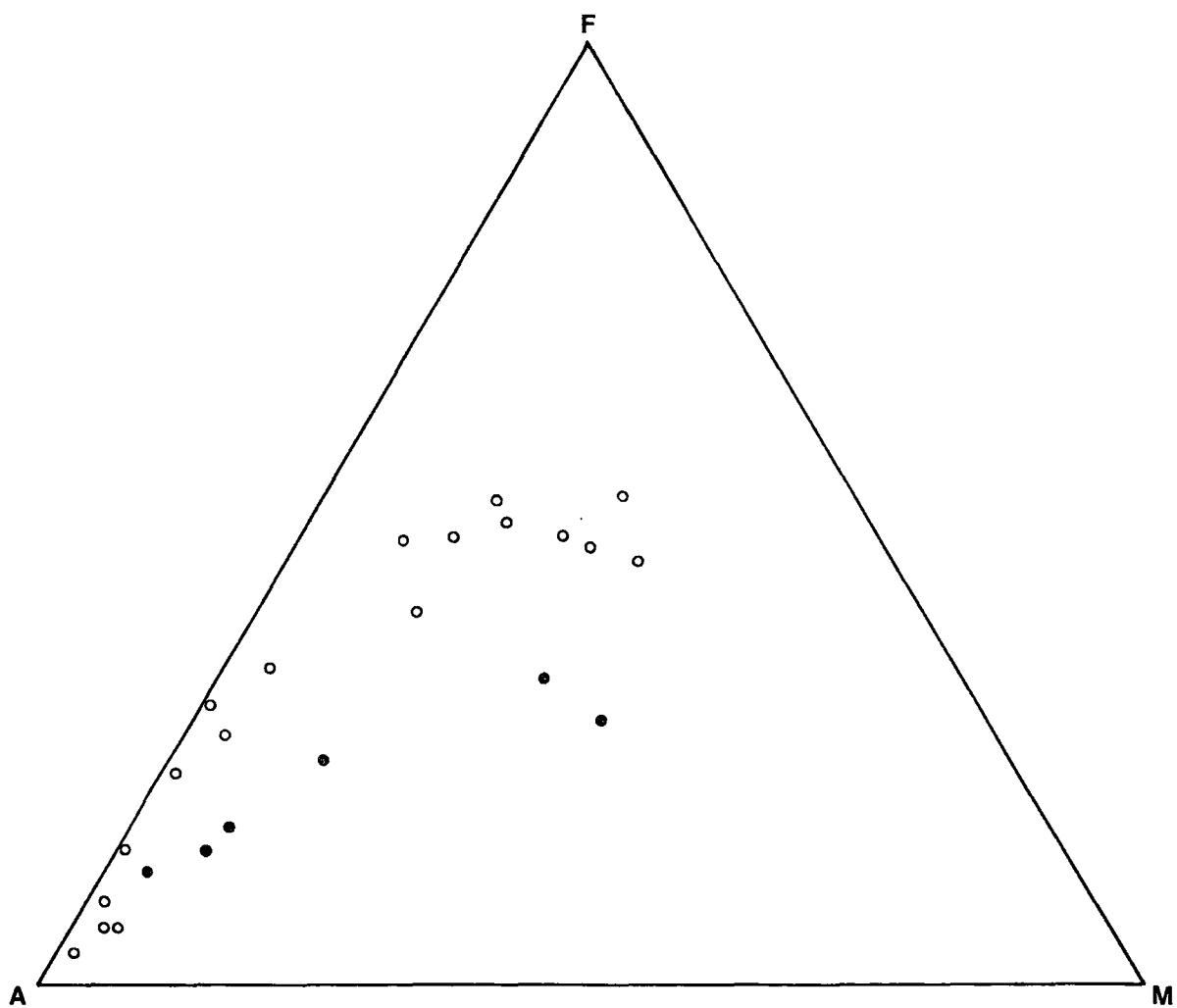
Differentiating liquids can fractionate either towards peraluminous minima (oversaturated alkali rhyolites and undersaturated phonolites) or towards peralkaline minima (oversaturated peralkaline trachytes, comendites and pantellerites, or undersaturated ijolites) (Bailey and Schairer, 1964). The ultimate differentiates in the Nandewar province are peraluminous alkali rhyolites, as they are in the study area; with $Al_2O_3 > CaO + Na_2O + K_2O$.

The Nandewar rhyolites are thought to be differentiates from a common parent magma. This is also likely for the Christopher Island rocks, due to the major and minor element trends as described in Chapter 4.

The primary stages of emplacement of the Nandewar mafics was a quiet process, as exemplified by the lack of pyroclastics and other features indicative of an explosive eruption. This is in direct contrast to the initial eruptives of the study area which are dominantly trachytic pyroclastics. The difference could be due to varying volatile contents of the two suites and overall composition, with the explosive eruption of the agglomerate in the study area being due, at least in part, to high volatile pressure.

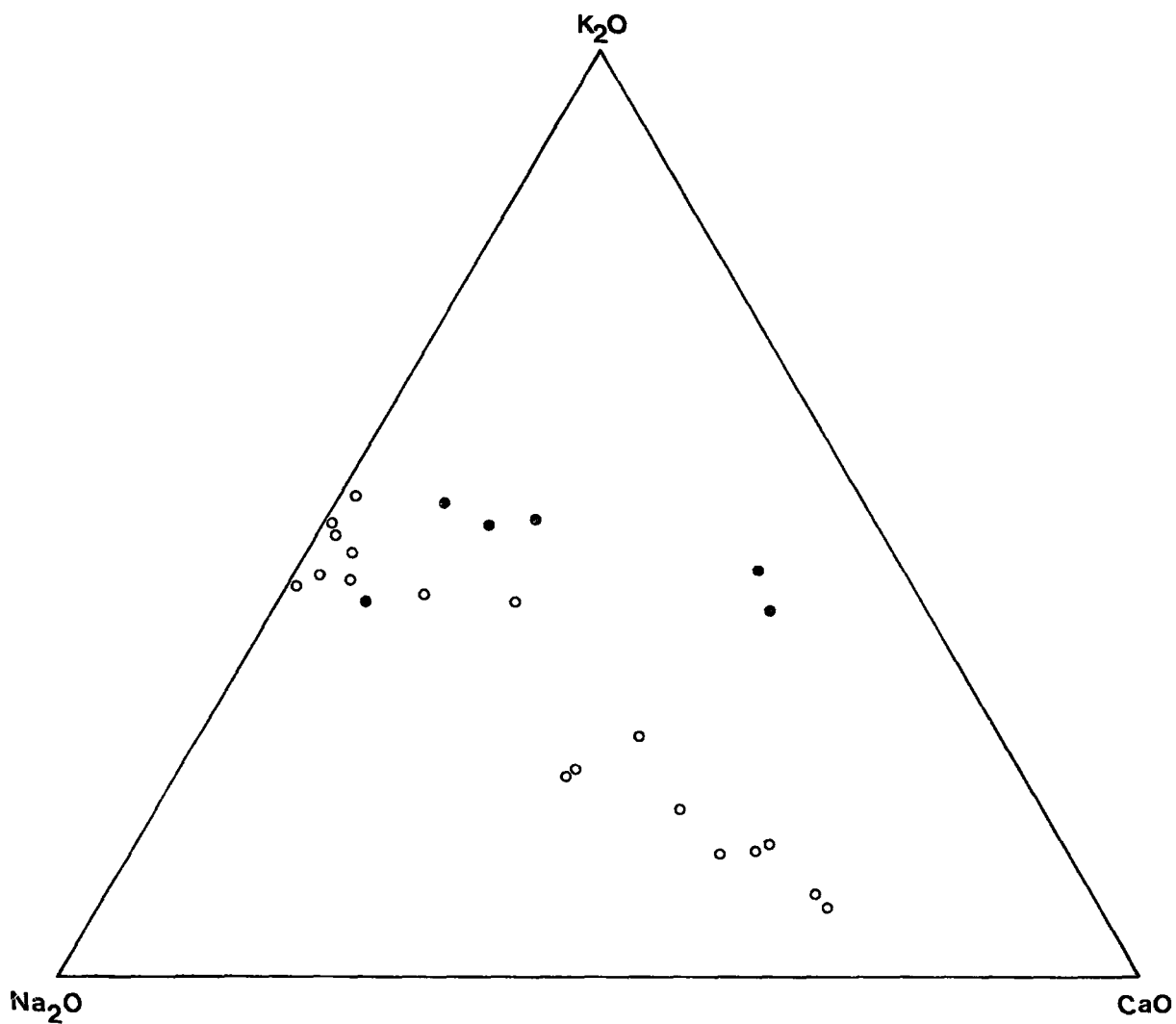
This pressure later appears to have diminished, as felsic pyroclastics were not observed in the study area.

Figure 7: Comparison of Nandewar Volcanics with Christopher Island Volcanics of Thesis Area



- Christopher Island Volcanics
- Nandewar Volcanics

Figure 8: Comparison of Nandewar Volcanics and Christopher Island Volcanics



- Nandewar Volcanics
- Christopher Island Volcanics of Study Area

CHAPTER SIX

CONCLUSIONS

It is apparent, through mineralogy, petrology, and chemistry that the Christopher Island Rocks of the study area represent a series of continental alkalic eruptions originating from a source deep within the mantle. It is thought that large scale regional faults acted as zones of weakness for the upward passage of magma. Alteration of the country rock, the 307 formation, appears to be related to the volcanism, and is likely hydrothermal.

Field relationships indicate at least one cycle of volcanism, possibly two within the study area.

Volcanism commenced with the explosive eruption of large amounts of pyroclastics; agglomerate proximal to the vent, lapilli tuffs and tuffs in the more distal areas. The agglomerate and other pyroclastics show large amounts of reworked epiclastic material, local scouring and reworking, gradation into bedded volcanoclastic deposits, all of which are typical of volcanic deposits. The presence of scouring and bedding implies, to a certain extent a subaqueous environment of deposition, likely fluvial or lacustrine.

The nature of the agglomerate is consistent over the entire area. Mineralogically the agglomerate remains

consistent; a phlogopite-phyric trachytic rock, commonly rich in epiclastic material.

The bombs and lapilli within the pyroclastics correspond mineralogically and chemically to the phlogopite trachytes, indicating contemporaneous effusion. Toward the more distal areas, the agglomerate becomes significantly richer in epiclastic material, the bombs decrease in size and finally are no longer evident.

At a later stage the magma source produced a series of flows increasingly more Si and Al rich and Fe, Mg, Ca and K poor. Iron, magnesium, calcium and potassium were depleted with increased differentiation. A trend towards subalkalinity appears in the final stages of volcanism, with the rocks becoming relatively depleted in the alkalies Na and K, with respect to Si and Al content.

Within the study area there is a wide variety of volcanoclastic deposits, but certain characteristics are common to most deposits and were used to determine age relationships. In particular unusual brown k-spar fragments were found in abundance in many of the arkoses. The brown k-spar, believed to be volcanic in origin, also occurs in the local syenites, and so dates any deposits in which it occurs as being the same age, or younger, than the volcanics. To a certain extent sorting and rounding can also be related to the age of the deposit relative to volcanism.

The presence of volcanic fragments, and their state upon deposition, whether molten or solid, is also diagnostic of age relationships, and proximity to the vent. Shards, pumice fragments, and lapilli are all common in the local volcanoclastics, sometimes reworked, sometimes fresh, having obviously been molten upon deposition.

Well sorted, fine grained wackes in the study area showing excellent thin laminar bedding indicate a different environment of deposition than the majority of the volcanoclastics. They are thought to represent basin deposits distal to the vent, and are significantly younger than the other volcanics. They show variations in strike and dip, indicating perhaps a slight unconformity between the two. Rare phlogopite laths are also present, in a surprisingly fresh, unaltered state.

The fine pale green ash associated with the pyroclastics and several of the proximal volcanoclastics is not evident.

Proximal to the vent, several of the volcanoclastic deposits are most likely lahar type deposits, and are probably younger than the agglomerate because of a lack of bombs within the deposits. Many scours are present, infilled with coarse well rounded cobbles and sandy material. Many of the cobbles are quartz. The source of this quartz is not positively known, but it likely originated

in the Archaean basement, within large quartz veins common to the area.

Other deposits show a jumble of consolidated blocks of similar composition to the matrix. These deposits are almost certainly slump deposits, occurring about the flanks of the volcano, triggered by small tremors associated with the volcanic activity.

In summary, intermediate volcanics intruded a continental alluvial fan deposit. The initial phase(s) was (were) explosive and followed by flows. Differentiation of a parent magma resulted in successively more felsic eruptions and intrusions. Typically significant deposits of volcanoclastics also occur, in the immediate vicinity, and are probably fluvial and lacustrine in nature. Later deposits, the volcanoclastic wackes, evidently originated in a basin type environment. The area is cut by a diabase dyke, one of many occurring as swarms in the Canadian Shield.

REFERENCES

- ABBOTT, M. J., 1969. Petrology of the Nandewar volcano, N.S.W., Australia. *Contrib. Mineral. Petrol.* Vol. 20, pp. 115-134.
- BAILEY, D. K. and SCHAIRER, J. R., 1966. The System $\text{Na}_2\text{O}-\text{Al}_2\text{O}_3-\text{Fe}_2\text{O}_3\text{SiO}_2$ at 1 atm and the petrogenesis of Alkaline Rocks. *J. Petrol.* Vol. 7, pp. 114-170.
- CARMICHAEL, I. S. E., TURNER, F. J. and VERHOOGEN, J., 1974. "Igneous Petrology" McGraw-Hill Co., New York.
- CARMICHAEL, I. S. E., 1965. Trachytes and their feldspar phenocrysts. *Mineral. Mag.* Vol. 34, pp. 107-125.
- CHARLES, R. W., 1977. The Phase equilibria of intermediate compositions on the pseudobinary $\text{Na}_2\text{CaMg}_5\text{Si}_8\text{O}_{22}(\text{OH})_2 - \text{Na}_2\text{CaFe}_5\text{Si}_8\text{O}_{22}(\text{OH})_2$. *Am. J. Sci.*, Vol. 277, No. 5, pp. 594-625.
- CHARLES, R. W., 1974. The physical properties of the Mg-Fe Richerites. *Am. Mineralogist*, Vol. 59, pp. 518-528.
- CURRIE, K. L., 1976. The Alkaline Rocks of Canada. G.S.C. Bull 239, 228 p.
- DONALDSON, J. A., 1967. Study of the Dubawnt Group. G.S.C. Paper 67-1, pp. 23-25.
- DONALDSON, J. A., 1966. Study of the Dubawnt Group. G.S.C. Paper 66-1,
- DONALDSON, J. A., 1964. The Dubawnt Group, districts of Keewatin and MacKenzie. G.S. C. Paper 62-20,

- EADE, K. E., 1976. Geology of Tulemalu Lake map-area
65J, district of Keewatin. G.S.C. Paper 76-1A.
pp. 379-380.
- EADE, K. W. and BLAKE, D. H., 1977. Geology of Tulemalu
Lake map-area. G.S.C. Paper 77-1A, pp. 209-211.
- FAHRIG, W. F. and WANLESS, R. K., 1963. Age and Significance
of Diabase Dyke Swarms of the Canadian Shield.
Nature, Vol. 200, pp. 934-937.
- FRASER, J. A. and HEYWOOD, W. W. (Eds.), 1978. "Metamorphism
in the Canadian Shield". G.S.C. Paper 78-10.
- IRVINE, T. N. and BARAGAR, W. R. A., 1971. A guide to the
chemical classification of the common volcanic rocks.
C.J.E.S., Vol. 8, pp. 523-548.
- JOHNSON, R. W. (Ed.), 1976. "Volcanism in Australasia"
Elsevier Scientific Publishing Co., New York.
- KING, B. C., 1960. Alkaline Rocks of Eastern and Southern
Africa. *Science Progress*, Vol. 48, pp. 298-321;
504-524; 709-720.
- LeCHEMINANT, A. N., LAMBERT, M. B., MILLER, A. R. and
BOOTH, G. W., 1979. Tebesjuak Lake Map Area, district
of Keewatin. G. S. C. Paper 79-1A, pp. 179-186.
- LeCHEMINANT, A. N. and MILLER, A. R., 1978. Five Types of
Uranium occurrence studied in Baker Lake basin.
Northern Miner, Nov. 30/78.

- LeCHEMINANT, A. N., BLAKE, D. H., LEATHERBARROW, R. W. and deBIE, L., 1975. Thirty-mile lake and MacQuoid Lake Map Areas, District of Keewatin. G.S.C. Paper 76-1A, pp. 383-386.
- LEEMAN, W. P. and ROGERS, J. J. W., 1970. Late Cenozoic alkali-olivine basalts of the Basin-Range province, U.S.A. Contrib. Mineral. Petrol. Vol. 25, pp. 1-24.
- MACDONALD, G. A., 1972. "Volcanoes" Prentice-Hall of Canada Ltd., Toronto.
- MACDONALD, R., BAILEY, D. K. and SUTHERLAND, D. S. , 1970. Oversaturated Peralkaline Glassy Trachytes from Kenya. J. Petrol. Vol. 11, pp. 507-517.
- ROSS, C. S. and SMITH, R. L., 1961. Ash-flow tuffs: Their Origin Geologic Relations and Identification. U.S.G.S. Professional Paper 366.
- TAYLOR, S. R., 1956. Some anomalous K/Rb ratios in igneous rocks and their petrological significance. Geochim. Cosmochim. Acta, Vol. 10, pp. 224-229.
- THORNTON, G. P. and TUTTLE, O. F., 1960. Chemistry of igneous rocks. J. Differentiation Index. Am. J. Sci., Vol. 258, pp. 664-684.
- WALKER, G. P. L., 1972. Crystal Concentration in Ignimbrites. Contr. Mineral. Petrol., Vol. 36, pp. 135-146.
- WANLESS, R. K. and EADE, K. E., 1975. Geochronology of Archaean and Proterozoic rocks in southern district of Keewatin. C.J.E.S. Vol. 12, pp. 45-114.

- WEAVER, S. D., SCEAL, J. S. C. and GIBSON, I. L., 1972.
Trace Element Data Relevant to the Origin of Trachytic
and Pantellerite lavas in the East African Rift
System. *Contrib. Mineral. Petrol.* Vol. 36, pp. 181-194.
- WILCOCKSON, W. H., 1964. Some aspects of east African
vulcanology. *Nature*, Vol. 203, No. 4948, 949 p.
- WRIGHT, G. M., 1967. Geology of the Southeastern Barren
Grounds, parts of the Districts of MacKenzie and
Keewatin. (Operations Keewatin, Baker, Thelon)
G.S. C. Mem. 350.
- WRIGHT, G. M., 1955. Geological notes on central District
of Keewatin, N.W. T. G. S. C. Paper 55-17.
- YODER, H. S. and EUGSTER, H. P., 1954. Phlogopite synthesis
and stability range. *Geochim. Cosmochim. Acta*,
157 p.

APPENDIX

Table 1: Major and Minor Elements Normalized Results (to 100%)

SAMPLE	SiO ₂	Al ₂ O ₃	Fe ₂ O ₃	MgO	CaO	Na ₂ O	K ₂ O	TiO ₂	MnO	P ₂ O ₅
K21-1	65.27	15.44	3.95	2.26	2.33	3.87	6.15	.43	.04	.26
K21-2	72.13	15.08	1.40	0.44	0.86	5.45	4.32	.23	.02	.07
K17-2	69.02	14.98	2.29	1.14	1.86	4.29	5.85	.33	.05	.19
K1-1	71.79	14.87	1.69	0.94	1.02	4.02	5.33	.23	.02	.09
K14-8	56.39	12.87	7.34	6.66	6.50	2.00	6.65	.76	.07	.77
K21-4	51.04	15.36	13.36	5.92	8.08	2.13	1.53	2.03	.19	.36
K2-2	59.23	11.60	5.91	7.66	6.90	1.60	5.62	.64	.07	.77

Table 2: Major and Minor Elements Normalized Results
 Corrected for $\text{Fe}_2\text{O}_3 \rightarrow \text{FeO} + \text{Fe}_2\text{O}_3$ with loss on ignition

SAMPLE	SiO_2	Al_2O_3	Fe_2O_3	FeO	MgO	CaO	Na_2O	K_2O	TiO_2	MnO	P_2O_5	L.O.I.
21-1	63.47	15.02	2.11	1.73	2.20	2.27	3.76	5.98	.42	.03	.25	2.76
21-2	71.30	14.91	1.38	0	.43	.85	5.39	4.27	.22	.02	.07	1.15
17-2	67.63	14.68	1.86	0.38	1.12	1.83	4.21	5.74	.32	.05	.18	2.01
1-1	70.76	14.65	1.66	0	.93	1.00	3.96	5.25	.22	.02	.09	1.44
14-8	53.18	12.14	2.68	4.24	6.29	6.13	1.88	6.27	.71	.07	.73	5.69
21-4	49.62	14.93	4.42	8.57	5.75	7.86	2.08	1.49	1.97	.19	.35	2.78
2-2	55.80	10.93	2.46	3.11	7.22	6.50	1.51	5.30	.61	.07	.73	5.79

K2-2 corrected for epiclastic quartz grains

Assuming 10% epiclastic quartz grains (with L.O.I.)

K2-2	50.08	12.14	2.73	3.46	8.02	7.22	1.68	5.89	.68	.08	.81	6.43
------	-------	-------	------	------	------	------	------	------	-----	-----	-----	------

(without L.O.I.)

K2-2	54.70	12.89	2.80	3.77	8.51	7.67	1.78	6.24	.71	.08	.85	
------	-------	-------	------	------	------	------	------	------	-----	-----	-----	--

Assuming 15% epiclastic quartz grains (with L.O.I.)

K2-2	48.00	12.85	2.89	3.65	8.49	7.65	1.78	6.24	.72	.08	.86	6.81
------	-------	-------	------	------	------	------	------	------	-----	-----	-----	------

(without L.O.I.)

K2-2	52.04	13.65	2.96	3.99	9.01	8.12	1.89	6.61	.75	.08	.91	
------	-------	-------	------	------	------	------	------	------	-----	-----	-----	--

Table 3: Trace Element Data (ppm)

SAMPLE	RB	SR	Y	ZR	NB	BA
K1-1	173	691	20	265	19	802.2
K14-8	250	1193	13	186	10	2480.6
K17-2	203	551	18	331	22	1436.6
K21-1	274	867	18	274	26	2559.3
K21-2	125	732	4	233	18	1813.1
K2-2 *	268	1919	18	616	10	3322.1
K21-4	109	564	32	172	13	697.0

	K_2O/Na_2O	SiO_2
K21-1	1.59	65.27
K21-2	0.79	72.13
K17-2	1.36	69.02
K1-1	1.33	71.79
K14-8	3.33	56.39
K2-2	3.51	59.23

Table 4: CIPW Norm No FeO or LOI Correction

MINERAL	K21-1	K21-2	K17-2	K1-1	K14-8	K21-4	K2-2
Calcite	0	0	0	0	0	0	0
Apatite	.602	.162	.440	.209	1.784	.834	1.789
Ilmenite	.086	.043	.107	.043	.150	.406	.150
Sphene	.945	.509	.672	.509	1.672	4.456	1.377
Orthoclase	35.345	25.530	34.572	31.499	39.300	9.042	33.213
Albite	32.747	46.117	36.301	34.017	16.924	18.024	13.539
Anorthite	6.596	3.087	4.342	3.750	6.500	27.833	7.872
Magnetite	0	0	0	0	0	0	0
Hematite	3.950	1.400	2.290	1.690	7.340	13.360	5.910
Quartz	12.405	21.749	17.314	24.829	2.095	9.810	8.989
Total Diopside	1.113	0	2.096	0	14.284	2.786	15.086
Wo	.597	0	1.124	0	7.662	1.495	8.092
En	.516	0	.972	0	6.622	1.292	6.994
Fe	0	0	0	0	0	0	0
Total Hypersthene	5.112	1.096	1.867	2.341	9.963	13.451	12.082
Enstatite	5.112	1.096	1.867	2.341	9.963	13.451	12.082
Corundum	0	.308	0	1.114	0	0	0
Σ100							
Alkalies A	61.738	84.152	74.724	78.047	38.190	15.955	34.728
Iron F	24.338	12.059	16.875	14.107	32.406	58.239	28.427
Magnesium M	13.925	3.790	8.401	7.846	29.404	25.806	36.845

Table 5: CIPW Norm with Both FeO correction and LOI added for CO₂

MINERAL	K21-1	K21-2	K17-2	K1-1	K14-8	K21-4	K2-2
Calcite	3.464	1.105	2.844	1.326	9.227	6.322	9.887
Apatite	.579	.162	.417	.209	1.691	.811	1.691
Ilmenite	.798	.043	.608	.043	1.348	3.742	1.159
Sphene	0	.485	0	.485	0	0	0
Orthoclase	35.540	25.235	33.922	31.026	37.054	8.806	31.322
Magnesite	2.370	.899	1.456	1.642	3.129	0	2.764
Albite	31.817	43.290	35.624	33.509	15.908	17.601	12.777
Anorthite	0	0	0	0	0	19.136	0
Corrundum	2.362	1.873	1.542	2.453	2.261	2.883	2.709
Magnetite	3.059	0	.460	0	3.886	20.908	3.567
Hematite	0	1.380	1.542	1.660	0	0	0
Quartz	16.758	25.050	20.540	27.267	9.039	14.562	16.665
Total Olivine	0	0	0	0	0	0	0
Forst.	0	0	0	0	0	0	0
Fayal.	0	0	0	0	0	0	0
Total Diopside	0	0	0	0	0	0	0
Wo	0	0	0	0	0	0	0
En	0	0	0	0	0	0	0
Fs	0	0	0	0	0	0	0
Hypersthene	3.453	0	1.056	.361	16.468	15.244	17.491
Enstatite	2.657	0	1.056	.361	11.939	14.319	14.689
Ferrosillite	.796	0	0	0	4.530	.924	2.801
Sodium Carb.	0	.469	0	0	0	0	0
A	61.724	84.220	74.756	78.051	38.155	11.049	34.745
F	24.335	12.031	16.829	14.068	32.397	71.154	28.418
M	13.942	3.749	8.415	7.881	29.448	17.796	36.837

Table 6: Data for AFM Diagrams
(totals recalculated to 100%)

	F	A	M
K21-1	24.3%	61.7%	13.9%
K21-2	12.1%	84.2%	3.8%
K17-2	16.9%	74.7%	8.4%
K1-1	14.1%	78.0%	7.8%
K14-8	32.4%	33.2%	29.4%
K2-2	28.4%	34.7%	36.9%

	F	A	M
K21-1	49.8%	31.3%	18.9%
K21-2	40.6%	51.3%	8.1%
K17-2	48.8%	35.8%	15.5%
K1-1	51.4%	38.8%	9.8%
K14-8	43.9%	13.2%	42.9%
K2-2	39.8%	14.2%	46.0%

Table 7: Cation Norm Results - AFM Data

	a) Without CO ₂ (LOI)			b) With CO ₂ (LOI)		
	A	F	M	A	F	M
K21-1	62.6	23.3	14.1	62.6	23.3	14.1
K21-2	85.2	11.0	3.8	85.2	11.0	3.8
K17-2	75.8	15.7	8.5	75.8	15.6	8.5
K1-1	79.2	12.9	8.0	79.2	12.8	8.0
K14-8	38.7	31.6	29.8	38.6	31.5	29.8
K21-4	16.3	57.4	26.3	11.6	69.8	18.6
K2-2	34.4	29.4	36.3	35.2	27.5	37.3

Table 8: Cation Norms (Mol %) without CO₂ (L.O.I.)

MINERAL	K21-1	K21-2	K17-2	K1-1	K14-8	K21-4	K2-2
Quartz	11.06	19.84	15.98	22.86	0	5.19	6.53
Corundum	0	.05	0	.93	0	0	0
Orthoclase	36.23	25.31	34.43	31.49	39.27	9.25	33.08
Albite	34.65	48.53	38.38	36.10	17.95	19.57	14.31
Anorthite	6.59	3.78	4.33	4.47	6.51	28.50	7.85
Leucite	0	0	0	0	0	0	0
Nepheline	0	0	0	0	0	0	0
Diopside	1.95	0	2.90	0	13.48	5.43	14.55
Hedenbergite	.25	0	0	0	3.08	2.67	2.44
Enstatite	5.25	1.20	1.69	2.60	11.15	14.01	13.80
Ferrosilite	.67	0	0	0	2.55	6.89	2.32
Forsterite	0	0	0	0	.37	0	0
Fayalite	0	0	0	0	.08	0	0
Magnetite	2.22	0	.38	0	2.89	4.83	2.62
Ilmenite	.60	.03	.46	.03	1.06	2.89	.89
Calcite	0	0	0	0	0	0	0
Hematite	0	.97	1.05	1.18	0	0	0
Apatite	.54	.15	.40	.19	1.16	.77	1.61
Augite	2.20		2.90	0	16.55	8.10	16.99
Hypersthene	5.92	1.20	1.69	2.60	13.70	20.90	16.12
Plagioclase	41.23	52.31	42.71	40.57	24.46	48.07	22.16
Rutile		.14		.14			
Olivine					.45		
Mg/Fe ratio	88.7	100	100	100	81.4	67.0	85.6
Mod. Lar. Ind.	12.3	13.9	13.6	14.3	5.6	-.1	4.3
Diff. Ind.	81.9	93.7	88.8	90.5	57.2	34.0	53.9

Table 9: Cation Norms (Mol %) Including LOI Results - Substituted in as CO₂ value

MINERAL	K21-1	K21-2	K17-2	K1-1	K14-8	K21-4	K2-2
Quartz	15.36	21.73	18.86	25.18	8.25	12.79	15.21
Corundum	2.55	1.54	1.67	2.67	2.43	2.99	2.92
Orthoclase	34.94	24.95	33.60	30.91	36.48	8.34	30.85
Albite	33.39	47.86	37.46	35.43	16.63	17.70	13.36
Anorthite	0	0	0	0	0	18.13	0
Leucite	0	0	0	0	0	0	0
Nepheline	0	0	0	0	0	0	0
Diopside	0	-.43	0	0	0	0	0
Hedenbeigite	0	0	0	0	0	0	0
Enstatite	2.91	0	1.16	.67	13.03	15.05	16.04
Ferrosialite	.66	0	0	0	3.76	.74	2.33
Forsterite	0	0	0	0	0	0	0
Fayalite	0	0	0	0	0	0	0
Magnetite	2.18	0	.33	0	2.76	14.29	2.53
Ilmenite	.58	.03	.44	.03	.97	2.60	.84
Calcite	6.90	2.88	5.04	3.63	14.17	6.66	14.43
Hematite	0	0.95	1.07	1.15	0	0	0
Apatite	.52	.14	.37	.19	1.51	.69	1.51
Augite	0	-.43	0	0	0	0	0
Hypersthene	3.58		1.16	.67	16.79	15.79	18.37
Plagioclase	33.39	47.86	37.46	35.43	16.63	35.84	13.36
Wollastonite		.22					
Rutile		.14		.14			
Mg/Fe ratio	81.4	100	100	100	7.76	95.3	87.3
Mod. Lar. Ind.	11.9	13.8	13.3	14.1	5.3	-.1	4.1
Diff. Ind.	83.7	94.5	89.9	91.5	61.4	33.8	59.4
FIELD NAME	FELSITES			→ TRACHYTE DIABASE TUFF			

40

Table 10: Data for AN-AB'-OR Diagrams Normalized to 100%

	AN	AB'	OR
K21-1	8.5	44.7	46.8
K21-2	4.8	62.5	32.6
K17-2	5.6	49.8	44.5
K1-1	6.2	50.1	43.7
K14-8	10.2	28.1	61.6
K21-4	49.7	34.1	16.1
K2-2	14.2	25.9	59.9

Table 11: Data for OL'-NE'-Q' Diagrams Normalized to 100%
with LOI

	OL'	NE'	Q'
K21-1	3%	63.3	33.7
K21-2	0	66.1	33.9
K17-2	.89	64.1	35.0
K1-1	.82	34.7	64.5
K14-8	30.2	23.9	45.8
K21-4	26.0	23.3	50.7
K2-2	28.2	16.4	55.5

without LOI

	OL'	NE'	Q'
K21-1	8.6	40.3	51.1
K21-2	1.3	41.9	56.8
K17-2	2.3	41.1	56.6
K1-1	3.2	35.2	61.6
K14-8	33.4	33.5	33.0
K21-4	34.3	25.7	40.0
K2-2	32.7	23.2	44.1

LIST OF SAMPLES, THIN SECTIONS and XRF (see also Plate 2)

SAMPLE

K1-1	alkali rhyolite	t.s. & XRF
K1-2	syenite	
K1-3	syenite	
K2-1	Agglomerate	
K2-2	Tuff	t.s. & XRF
K4-1	syenite	
K5-1	Lapilli Tuff	
K5-2	alkali rhyolite	t.s.
K6-1	arkose (307)	
K7-1	volcaniclastic	t.s.
K7-2	arkose (307)	
K9-1	syenite	t.s.
K9-2	diabase	
K9-3	phlogopite trachyte	t.s.
K10-1	alkali rhyolite	
K10-2	syenite	
K10-3	volcaniclastic	t.s.
K10-4	volcaniclastic	t.s.
K10-5	volcaniclastic	
K10-6	trachyandesite	
K10-7	alkali rhyolite	
K10-8	volcaniclastic	

SAMPLE

K11-1	volcaniclastic wacke	t.s.
K13-1	~ trachyandesite	
K13-2	volcaniclastic wacke	
K13-3	phlogopite trachyte	t.s.
K14-1	phlogopite trachyte	
K14-2	volcaniclastic wacke	
K14-3	Tuff	
K14-4	volcaniclastic	t.s.
K14-5	Tuff	t.s.
K14-6	phlogopite trachyte	
K14-7	phlogopite trachyte	t.s.
K18-8	phlogopite trachyte	t.s. & XRF
K16-1	trachyte	
K16-2	diabase	
K17-1	arkose (307)	t.s.
K17-2	alkali rhyolite	XRF
K18-1	arkose (307)	t.s.
K19-1	arkose (307)	
K20-1	syenite	t.s.
K21-1	alkali rhyolite	XRF
K21-2	alkali rhyolite	XRF
K21-3	arkose (307)	
K21-4	diabase	XRF

SAMPLE

K21-5	arkose (307)	t.s.
K21-7	Tuff	t.s.
K23-1	volcaniclastic	
K23-2	syenite	t.s.